Chemical Science

ROYAL SOCIETY OF CHEMISTRY

REVIEW

View Article Online
View Journal | View Issue



Cite this: *Chem. Sci.*, 2025, **16**, 3408

# Effects of oxygen vacancies on hydrogenation efficiency by spillover in catalysts

Lijuan Xie,[a] Jinshan Liang,[a] Lizhi Jiang *[a] and Wei Huang*[abc]

Hydrogen spillover is crucial for hydrogenation reactions on supported catalysts. The properties of supports have been reported to be very important for affecting hydrogen spillover and the subsequent hydrogenation process. The introduction of oxygen vacancies offers a promising strategy to enhance efficiency of catalysts. Recent advanced characterization and theoretical modeling techniques have provided us with increasing new insights for understanding hydrogen spillover effects. However, a comprehensive understanding of oxygen vacancy effects on hydrogen spillover and hydrogenation efficiency of catalysts is still lacking. This review focuses on the recent advances in support effects especially oxygen vacancy effects on improving the efficiency of catalysts from three process aspects including hydrogen dissociation, active hydrogen spillover, and hydrogenation by spillover. The challenges in studying the effects on hydrogenations by spillover on the supported catalysts are highlighted at the end of the review. It aims to provide valuable strategies for the development of high-performance catalytic hydrogenation materials.

Received 31st October 2024
Accepted 27th January 2025

DOI: 10.1039/d4sc07375d

rsc.li/chemical-science



## 1. Introduction

The development of effective catalysts is urgently demanded for the practical application of chemical synthesis, energy storage, and conversion technologies. It is known as a smart strategy to create new active sites to enhance efficiency for heterogeneous catalysts by spillover.[1–3] In catalysis, only the activated species spillover is important. Recent studies have highlighted the multifaceted role of metal oxide supports in catalytic hydrogenation. These supports not only facilitate the dissociation of $H_2$ but also act as "hydrogen reservoirs", absorbing and storing hydrogen atoms and releasing them under favorable conditions to sustain catalytic reactions.

A critical feature of metal oxide supports contributing to this process is the presence of oxygen vacancies. These vacancies have attracted significant attention due to their ability to modulate the electronic properties of metal oxide supports, thereby influencing their catalytic behavior. Cao *et al.* investigated the role of oxygen vacancies in $CeO_2$ using carbon dioxide hydrogenation as a model reaction.[4] Their findings provide

[a]*Strait Institute of Flexible Electronics (SIFE, Future Technologies), Fujian Normal University and Strait Laboratory of Flexible Electronics (SLoFE), Fuzhou, Fujian, 350117, China. E-mail: ifelzhjiang@fjnu.edu.cn*

[b]*Key Laboratory of Flexible Electronics & Institute of Advanced Materials, Nanjing Tech University, Nanjing, 211816, China. E-mail: vc@nwpu.edu.cn*

[c]*Frontiers Science Center for Flexible Electronics, Shaanxi Institute of Flexible Electronics (SIFE), Northwestern Polytechnical University (NPU), 127 West Youyi Road, Xi'an, 710072, China*

**Lijuan Xie**

*Lijuan Xie received her B.S. degree in environmental engineering from Fujian Agriculture and Forestry University in 2022, and is currently pursuing her MS degree at the Strait Institute of Flexible Electronics of Fujian Normal University. Her research interests focus on the mechanisms of hydrogen spillover and hydrogenation catalysis.*

**Lizhi Jiang**

*Lizhi Jiang received her PhD degree from Kyushu University in 2013. In 2021, she joined the Strait Institute of Flexible Electronics, Fujian Normal University, and became an associate professor. Her research interests focus on electronic properties of materials and mechanisms of catalysis on surfaces and interfaces of materials.*

direct evidence that surface oxygen atoms are integral to the activation of $H_2$, while oxygen vacancies accelerate the dissociation of $CO_2$, underscoring the unique catalytic roles of both surface oxygen and oxygen vacancies. Similarly, recent work by Wang *et al.* has demonstrated that oxygen-deficient tungsten oxide is a versatile and efficient catalyst for the hydrogenation of nitroaromatic hydrocarbons.[5,6] The study revealed that the catalytic activity of tungsten oxide is closely linked to the concentration of oxygen vacancies, with higher vacancy concentrations correlating with enhanced catalytic performance. Furthermore, oxygen vacancies alter the dissociation pathway of $H_2$, with one dissociated hydrogen atom bonding to a surface metal atom and the other to an adjacent oxygen vacancy site, thereby optimizing catalytic efficiency.[5] Despite these promising advancements, challenges such as slow hydrogen spillover rates, limited spillover distances, and insufficient adsorption capacities of the support materials continue to impede their industrial application, challenges that become especially acute when scaling these technologies for broader industrial deployment, where maintaining consistent performance and efficiency is paramount.[7,8]

The process of hydrogenation by spillover involves three primary processes: the dissociation of $H_2$ on the active metal, the migration of dissociated H on the "inert" support[9–13] and hydrogenation. Recent advancements in both experimental and computational methods have provided us with more evidence for deeper understanding of the process of hydrogenation by spillover, as the advent of advanced surface characterization techniques such as *in situ* spectroscopy and high-resolution electron microscopy has enabled researchers to observe, with unprecedented clarity, the dissociation of $H_2$ on active metal sites in real time, thereby providing direct and compelling evidence for the spillover phenomenon.[14] Furthermore, computational methods, particularly density functional theory (DFT) and molecular dynamics simulations, have proven indispensable for elucidating the migration pathways of dissociated hydrogen on inert supports while accurately predicting the energetics and kinetics of these processes.[15] These techniques have not only confirmed the existence of spillover hydrogen but have also yielded critical insights into the factors influencing their efficiency, including the properties of the support material, particle size, and the nature of the active metal. Despite these significant advancements, a conspicuous gap remains in the literature—a comprehensive and systematic review that summarizes these findings is still absent, a shortfall that, if addressed, would be invaluable for consolidating the current state of knowledge, identifying persistent challenges.

This review highlights recent progress in understanding the oxygen vacancy effects on hydrogenations by spillover on catalysts through the three important step processes (Fig. 1). We start to discuss the different types of hydrogen dissociation, and then briefly introduce the migration and reaction of active hydrogen species on various supports, and clearly summarize the typical factors affecting hydrogenation including oxygen vacancies. In conclusion, this review provides a comprehensive summary of the current research status and prospects of hydrogen spillover, aiming to offer new insights for the design and application of this phenomenon in catalytic processes.

## 2. Oxygen vacancies in metal oxides supports

Supported catalysts used in hydrogenation reactions typically consist of two main components: a metal phase and a support material. The metal phase, often composed of noble metals such as Pt, Pd, Rh, or Ru, is responsible for the adsorption and dissociation of hydrogen molecules, and is also as the active site for hydrogenation. The supports can usually be divided into reducible and irreducible materials. The dissociated hydrogens could then spill to the reducible support materials such as $CeO_2$ and $TiO_2$, which provide a platform for hydrogen atom migration and stabilize the active hydrogen species through various interactions.[10,12]

Metal oxide catalysts exhibit excellent activity, selectivity and stability in various redox reactions.[16–18] The redox performance of these catalysts is strongly influenced by the distribution and concentration of oxygen vacancies, which are considered key active sites within the oxide matrix. Oxygen vacancies can exist at both the surface and subsurface regions of the support material (Fig. 2), and they are critical for the activation and stabilization of hydrogen atoms. Surface oxygen vacancies are particularly significant due to their higher reactivity, as they directly influence the adsorption and activation of reactant molecules. In contrast, subsurface oxygen vacancies, situated several atomic layers beneath the surface, do not directly engage in reactions. However, they play a vital role in modulating the electronic structure of the catalyst by redistributing electrons, which can indirectly impact the overall catalytic performance.[19]

These oxygen vacancies not only act as active sites for hydrogen migration from the metal phase to the support but also influence the adsorption and activation of reactant molecules. The coordination environment around these vacancies, such as the number and distribution of neighboring metal cations, greatly affects their reactivity. Moreover, the migration

**Wei Huang**

*Wei Huang received his PhD from Peking University in 1992. In 1993, he began his postdoctoral research at the National University of Singapore. In 2001, he joined Fudan University, and then founded the Institute of Advanced Materials. In 2006, he was appointed as the Deputy President of the Nanjing University of Posts and Telecommunications. Then he was appointed as the President of Nanjing Tech University in 2012. Then he was appointed as the Deputy President of Northwestern Polytechnical University in 2017. His research interests include organic electronics and flexible electronics.*

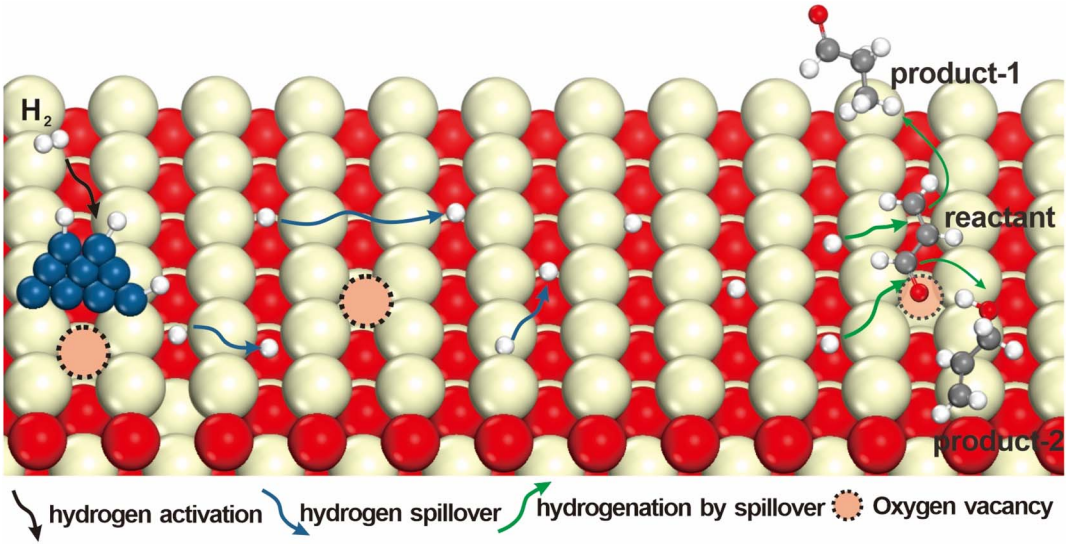


Fig. 1 Schematic diagram of the effects of oxygen vacancies on the hydrogenation efficiency of an unsaturated substrate in the case of acrolein. The elementary reactions typically occur in the following sequence: activation of $H_2$; transfer of active hydrogen and various hydrogenation reactions with unsaturated substrates. The presence of oxygen vacancies in surfaces facilitates effective hydrogenations.

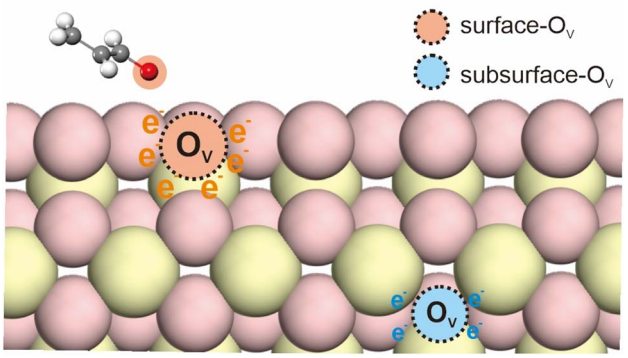


Fig. 2 Diagram of oxygen vacancy species on a metal oxide catalyst.

of oxygen vacancies within the support materials is essential for maintaining catalytic activity, as it influences the electronic structure of the catalyst and its overall stability. The following sections will discuss their coordination environments, and the mechanisms governing their migration. Understanding these factors is crucial for optimizing the efficiency of hydrogenation reactions.

### 2.1 Coordination environment of oxygen vacancies

In catalytic systems, particularly those involving metal oxides like $CeO_2$, the reactivity of oxygen vacancies is crucial for efficient catalytic processes. A highly reactive oxygen vacancy must balance the strong adsorption of reactant molecules with the effective desorption of product molecules. This delicate balance is significantly influenced by the local atomic and electronic environment surrounding the vacancy. For instance, in the fluorite structure of $CeO_2$, oxygen ions are typically tetrahedrally coordinated with $Ce^{4+}$ cations. Introducing structural asymmetry by doping with other metal cations can disrupt this symmetry (Fig. 3a), leading to a redistribution of electron density around the oxygen vacancies.[20] This redistribution may enhance the activity of the oxygen vacancy, allowing it to participate more efficiently in catalytic reactions and providing a new dimension for catalyst design.

$CeO_2$ and its derivatives are regarded as excellent active supports due to their abundant oxygen vacancies.[23] Recent advancements in the field have demonstrated that doping $CeO_2$ with various transition metals can strategically modify the electronic properties of these vacancies, thereby significantly enhancing the material's catalytic efficiency. In a study conducted by Yu *et al.*, low-cost doping ions with distinct d-band centers were introduced into $Pt/CeO_2(100)$ to create the $Pt/Ce–O_V–M$ interface.[21] This strategic doping alters the charge densities within the oxygen vacancies, as the doped ions influence the electronic effects at these sites (Fig. 3b). Notably, the transfer of electrons from $Pt_4$ clusters to the asymmetric $Ce–O_V–Y$ and $Ce–O_V–La$ sites was observed, with doping by Y and La demonstrating a marked enhancement in interfacial charge transfer. Further investigations revealed that when $O_2$ was adsorbed at the $Pt_4/Ce–O_V–Y$ site, there was significant electron depletion in the Y-4d orbital (Fig. 3c and d), which was corroborated by Bader charge analysis. This highlights the critical role of doping in modifying the electronic environment of oxygen vacancies, thus improving their ability to participate in catalytic reactions.

### 2.2 Migration of oxygen vacancies

The migration behavior of oxygen vacancies is a pivotal aspect of catalytic science, as the diffusion of these vacancies during catalytic reactions intricately affects the activity and stability of the catalyst.[24] In the context of transition metal oxides like $TiO_2$, oxygen vacancies play a crucial role in modulating the material's

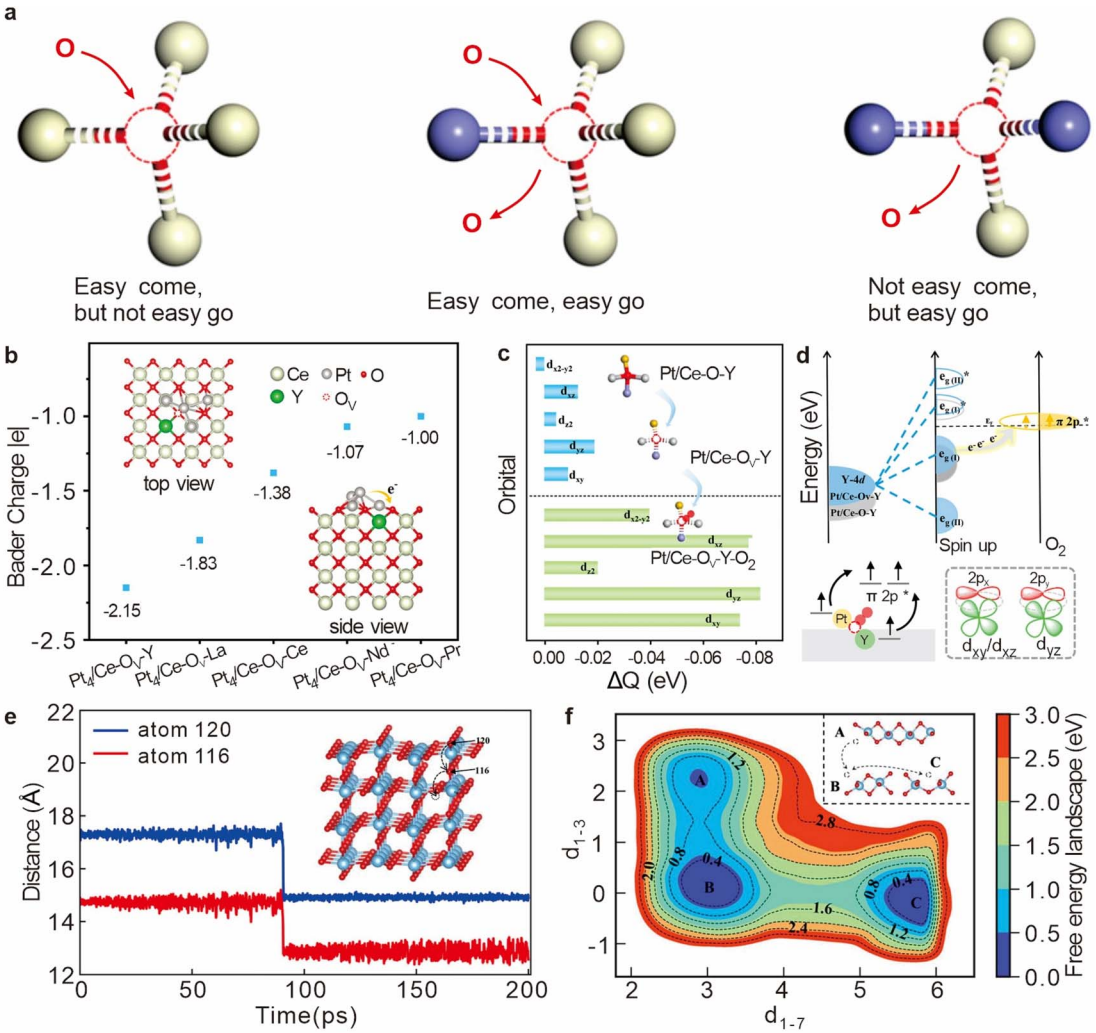


Fig. 3 (a) Schematic diagram of the relationship between the microstructure of an oxygen vacancy and its redox properties. Reproduced with permission. Reproduced from ref. 20. Copyright 2019 Wiley-VCH GmbH. (b) Bader charge of the $Pt_4$ cluster deposited onto different oxygen vacancy sites. (c) Variation of charge density due to oxygen vacancy formation and oxygen adsorption in $Pt_4/Ce-O_v-Y$ (d) Electronic modulation effect of Y doping in $Pt_4/Ce-O_V-Y$ on $O_2$ activation. Reproduced from ref. 21. Copyright 2024 American Chemical Society. (e) Vertical diffusion process of $O_V-5$ to the surface. (f) Free energy surface of $O_V-1$ diffusion at 330 K as a function of collective variables $d_{1-3}$ and $d_{1-7}$. Reproduced from ref. 22. Copyright 2023 American Chemical Society.

electronic and structural properties, which in turn influences its photocatalytic performance.

The introduction and precise control of oxygen vacancies in $TiO_2$ have been shown to enhance its photocatalytic efficiency, making it a subject of intense research. Studies such as those conducted by Wu *et al.* have employed advanced computational methods, including Deep Potential Molecular Dynamics (DPMD) and enhanced sampling techniques, to model the diffusion behavior of oxygen vacancies in $TiO_2$, particularly focusing on the rutile (110) surface.[22] By constructing a detailed Deep Potential (DP) model, the researchers were able to simulate the diffusion of oxygen vacancies both within the atomic layers and on the surface of $TiO_2$ (Fig. 3e). To further elucidate the diffusion mechanism of surface oxygen vacancies, Wu *et al.* utilized the Well-Tempered Metadynamics (WT-MetaD) method to reconstruct the free energy surface associated with the diffusion process at 330 K (Fig. 3f).[22] The analysis employed key coordinate variables (cv $d_{1-3}$ and $d_{1-7}$) to model the migration pathways, revealing distinct states (B and C) that correspond to oxygen vacancies at different locations on the surface. The findings showed that the diffusion of an oxygen vacancy from state B to state C in the [001] direction encounters a free energy barrier of approximately 1.43 eV. This barrier is indicative of the kinetic challenges involved in vacancy migration, which can influence the overall reactivity and efficiency of the catalytic process.

These insights into the kinetic and thermodynamic behavior of oxygen vacancies on $TiO_2$ surfaces contribute to a deeper understanding of how vacancy migration impacts catalytic activity. By manipulating the concentration, distribution, and mobility of oxygen vacancies, researchers can optimize the performance of $TiO_2$-based catalysts, making them highly

adaptable for specific applications in photocatalysis and other catalytic processes. The ability to fine-tune these factors offers significant potential for improving the selectivity and efficiency of catalytic reactions, thus enhancing the industrial applicability of $TiO_2$ and related materials.

# 3. Hydrogen activation

## 3.1 Hydrogen activation mechanism

The dissociation of $H_2$ on metal surfaces, a crucial step in catalytic hydrogenation, occurs through two primary pathways: homolytic and heterolytic dissociation.[25] Homolytic dissociation involves the symmetrical cleavage of the H–H bond, where each hydrogen atom binds to a metal center, typically favored in environments where metal atoms are closely spaced, as observed in transition metals like platinum and palladium (Fig. 4a). In contrast, heterolytic dissociation involves an asymmetric cleavage, with one hydrogen atom binding to the Lewis acidic metal center and the other associating with a nearby Lewis base, commonly seen in metal–support systems with electron-donating species (Fig. 4b).

The choice of dissociation pathway significantly impacts catalytic performance, influencing the overall activity, selectivity, and stability of the catalyst. Homolytic dissociation typically produces highly reactive metal-hydride species that, although effective in hydrogenation reactions, may also lead to side reactions if not carefully controlled. In contrast, heterolytic dissociation, by involving a base, generally enables more controlled and selective hydrogenation processes, especially when multifunctional catalysts leverage the base's properties to direct the reaction towards the desired products. To gain a deeper understanding of the dissociation mechanism, theoretical calculations including DFT are widely used to model the energy barriers and reaction pathways of different dissociation mechanisms. Computational methods provide insights into the microscopic mechanisms of the reactions, uncovering details that may not be fully understood through experimental observations alone.

It has been widely believed that hydrogen molecules dissociate into hydrogen atoms with a partial negative charge ($H^{\delta-}$) through homolytic cleavage on Pd particle catalysts.[26] However, when Pd atoms are individually dispersed in $Pd_1/TiO_2$ catalysts, no Pd–Pd pairs are available for the homolytic cleavage of $H_2$. DFT calculations conducted by Zheng *et al.* showed that $H_2$ adsorbed on $Pd_1$ readily splits into two H atoms, and one H atom migrates to a nearby oxygen atom forming an O–$H^{\delta+}$ bond, while the other H atom remains on Pd forming an $H^{\delta-}$ species.[27] This discovery not only challenges traditional understanding but also underscores the importance of studying hydrogen dissociation mechanisms in catalytic hydrogenation and hydrogen storage processes.

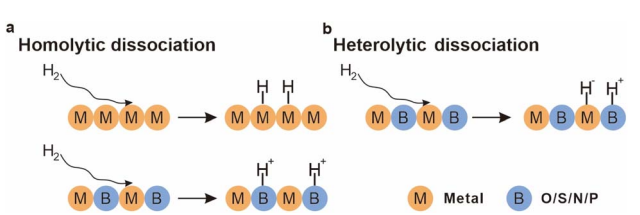


Fig. 4 (a) Illustration of $H_2$ homolytic dissociation pathways. (b) Illustration of $H_2$ heterolytic dissociation pathways.

## 3.2 Oxygen vacancy effects on hydrogen activation

The dissociation mode of hydrogen significantly influences the type and behavior of active hydrogen species, which in turn dictates the catalytic reaction pathway and product distribution. Recent studies have highlighted the potential of oxide catalysts in promoting heterolytic dissociation of hydrogen, and especially those located on the surface or at the metal–support interface, can shift the dissociation process, thereby enhancing the generation of active hydrogen atoms (Fig. 5a). Gong *et al.* reported that on the $CeO_2(110)$ surface, homolytic dissociation of $H_2$ into two OH groups is thermodynamically favorable, but becomes unstable as the concentration of surface oxygen vacancies increases. Meanwhile, on the $CeO_2(110)$ surface with moderate defects, heterolytic dissociation of $H_2$ into an $H^-$ atom at the oxygen vacancy site and an OH group is thermodynamically permissible. This is consistent with previous DFT calculations, which suggest that surface oxygen vacancies can enhance the stability of $H^-$ species.[28] Yang *et al.* discovered that the homolytic cleavage of hydrogen on $\alpha$-$Ga_2O_3$ occurs at the coordination-unsaturated $Ga^{3+}$ sites formed during the initial heterolytic dissociation process.[29] As shown in Fig. 5c, Ga–H and Ga–OH rapidly form and intensify simultaneously when $\alpha$-$Ga_2O_3$ is exposed to $H_2$, but the concentration of Ga–H continues to increase at a rate of 0.9 $nm^{-2}$ $min^{-1}$ after Ga–OH stabilization, with the final hydride-to-hydroxyl ratio reaching 5.6. Further DFT calculations revealed the dissociation behavior of $H_2$ on the oxygen-deficient $\alpha$-$Ga_2O_3(001)$ surface (Fig. 5d), the heterolytic dissociation of $H_2$ initially releases a significant amount of energy (1.65 eV), and the resulting hydrides migrate to neighboring O atoms to form hydroxyl groups, releasing an additional 0.58 eV of energy. Interestingly, the average dissociation energy of $H_2$ in the presence of adjacent hydroxyl groups is −0.46 eV (Fig. 5d), whereas the dissociation energy of $H_2$ without prior heterolytic cleavage is +0.28 eV, which indicates that heterolytic dissociation is a prerequisite for homolytic cleavage. This dual dissociation mechanism can significantly enhance the overall catalytic activity. This highlights the importance of designing catalysts that can selectively control the hydrogen dissociation pathway to optimize the catalytic process for specific reactions.

The dissociation capacity of hydrogen is a critical factor for determining the production rate of active hydrogen species in catalytic hydrogenation processes. This capacity is influenced not only by the inherent properties of the metal at the dissociation site but also by the characteristics of the support material. The interaction between metal particles and the support can significantly alter the electronic environment and the distribution of active sites, thereby enhancing or hindering hydrogen dissociation. Recent studies have shown that by carefully designing and engineering the catalyst's structure, researchers

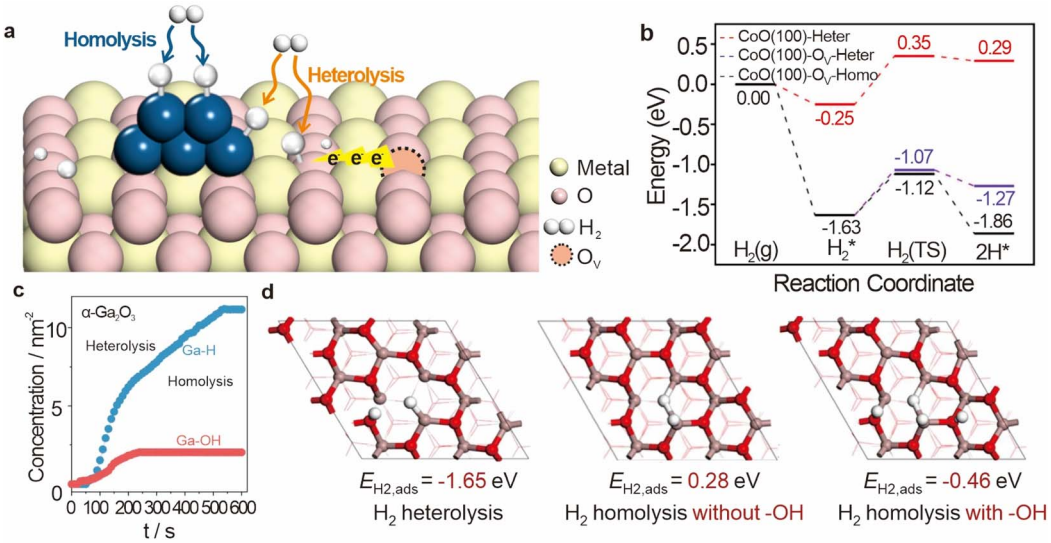


Fig. 5 (a) Mechanism of oxygen vacancies affecting hydrogen dissociation. (b) Calculated energy profiles of adsorption and dissociation of $H_2$. Reproduced from ref. 30. Copyright 2022 Springer Nature. (c) The evolution of surface Ga–H and Ga–OH over α-$Ga_2O_3$ samples with contact time of $H_2$ at 350 °C. (d) $H_2$ adsorption energy by homolytic dissociation over α-$Ga_2O_3$ (001). Reproduced from ref. 29. Copyright 2024 Springer Nature.

can significantly improve hydrogen dissociation efficiency. By combining spectral experiments and computational models, Wang *et al.* elucidated the promoting effect of a CoO shell with oxygen vacancies on the $H_2$ dissociation process.[30] They found that the heterolytic dissociation of $H_2$ on the CoO(100) surface required overcoming a potential barrier of 0.60 eV, but the presence of oxygen vacancies on the CoO(100)–$O_V$ surface made the adsorption and dissociation process (Fig. 5b) of $H_2$ more favorable; the heat absorption was reduced (0.36 eV) and the barrier was lower at 0.56 eV.

## 4. Hydrogen spillover process

### 4.1 Hydrogen spillover mechanism

The phenomenon of hydrogen spillover, initially discovered by Khoobiar during the hydrogen reduction of $WO_3$, marks a pivotal development in catalysis science.[31] Initially, hydrogen molecules are adsorbed onto the metal surface, where they undergo dissociation to form active hydrogen atoms. These hydrogen atoms then migrate from the metal surface to the metal–support interface, where they can diffuse across the support material, as hydrogen dissociation does not occur on the support itself. Importantly, hydrogen spillover is not confined to the support surface immediately adjacent to the activated metal; it can extend to other areas of the support. In cases where the composition of a secondary accepting surface differs from that of the initial surface, secondary spillover may take place, further facilitating hydrogen migration.[32,33] Despite decades of research, the underlying mechanisms of hydrogen spillover remain incompletely understood. An in-depth exploration of the spillover mechanism on various supports is essential for effectively leveraging this phenomenon to enhance catalytic performance. For supported metal catalysts, it is widely accepted that hydrogen spillover can efficiently occur on easily reducible oxide supports such as $WO_3$ and $TiO_2$.[15,34] These oxides facilitate the migration of hydrogen atoms across their surfaces, enhancing the catalytic activity of the supported metal particles. However, the possibility of hydrogen spillover on less reducible oxide supports, such as $SiO_2$ and $Al_2O_3$, has been a contentious topic in the academic community. This controversy stems from the inherent difficulty in experimentally observing hydrogen spillover on such supports due to their low reducibility and the challenges associated with visualizing this phenomenon.[9,35–38]

Traditional methods for studying hydrogen spillover have encountered significant limitations, particularly in the development of model systems with clearly separated catalytic functions. These challenges have hindered the direct observation and quantification of hydrogen spillover, complicating the understanding of its mechanisms. To address these challenges, Waiz Karim *et al.* developed an innovative approach by placing pairs of iron oxide and platinum nanoparticles on different supports, creating a model system with a distance gradient to directly observe the chemical transformations induced by hydrogen spillover (Fig. 6a).[10] This experimental setup provided direct and intuitive evidence for hydrogen spillover behavior on various supports, shedding light on the complex interplay between support materials and spillover phenomena. Additionally, the adsorption and migration mechanisms of hydrogen on $TiO_2$ and γ-$Al_2O_3$ were explored through first-principles simulations.[39,40] These computational studies revealed that the spillover barrier of hydrogen atoms (H*) to $TiO_2$ after separation is approximately 0.45 eV, indicating the feasibility of hydrogen spillover in this system (Fig. 6b). On the γ-$Al_2O_3$ support, the transfer of H* between adjacent alumina sites exhibited an activation energy barrier ranging from 1.15 eV

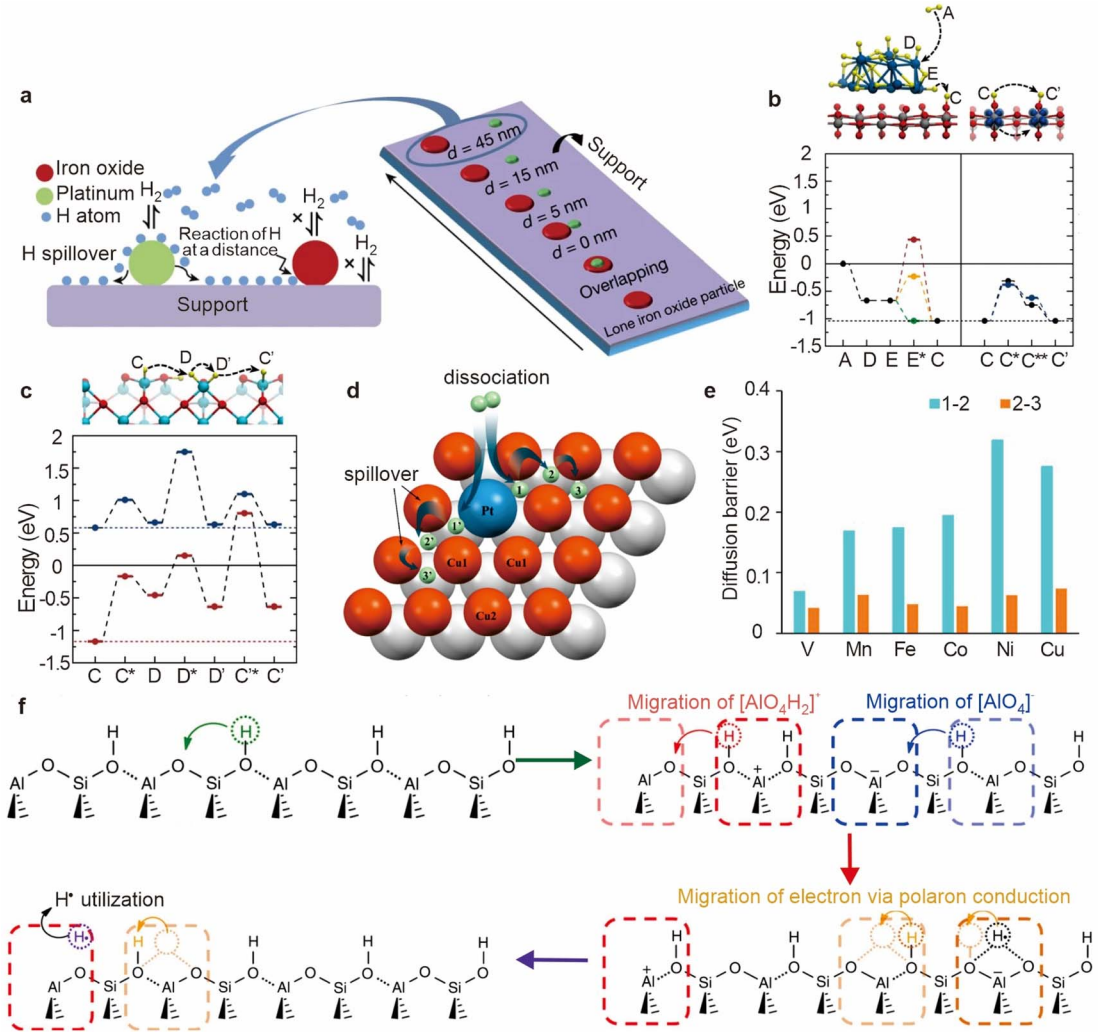


Fig. 6 (a) Scheme of hydrogen spillover from platinum to an iron oxide particle over a titanium oxide or aluminium oxide support. (b) Hydrogen dissociation on the platinum cluster and spillover to anatase titanium oxide. (c) Hydride mobility on γ-aluminium oxide. Reproduced from ref. 10. Copyright 2017 Springer Nature. (d) Schematic diagram of $H_2$ dissociation and hydrogen spillover on the $Pt_{1-x}$/Cu(111) surface. (e) Diffusion barrier of H over the catalyst surface. Reproduced from ref. 41. Copyright 2024 American Chemical Society. (f) Proposed mechanism for the hydrogen spillover. Reproduced from ref. 9. Copyright 2014 Springer Nature.

to 1.63 eV, depending on the degree of surface hydration (Fig. 6c).

These findings align with those of previous theoretical and experimental work,[42,43] confirming that the mobility of hydrogen on the surface of γ-$Al_2O_3$ is more restricted than on $TiO_2$. On irreducible oxide catalysts, such as silica–alumina ($SiO_2$–$Al_2O_3$), early research has identified Brønsted acid sites (BAS) and defect sites produced by surface hydroxyl groups as potential stabilizers for atomic hydrogen.[44,45] These sites are significant because they may stabilize atomic hydrogen, facilitating its migration across the catalyst surface. However, the mechanism by which atomic hydrogen migrates at these sites has not been systematically explored, leaving gaps in the understanding of this process.

Juhwan Im *et al.* made notable strides in this area by developing Pt/NaA zeolites with Pt clusters selectively embedded within the zeolite's micropore structure.[9] This novel material design provides an excellent platform for investigating the migration mechanism of atomic hydrogen in zeolites. As shown in Fig. 6f, at the bridge site of two oxygen atoms in the $[AlO_4]^-$ framework, the hydrogen radical (H•) is stabilized through the formation of a three-center bond (O–H–O). This three-center bond formation is driven by the presence of spatially localized unpaired electrons, also known as polarons, which induce a local structural distortion at the original BAS site $[AlO_4]^-H^+$. The unpaired electrons at the $[AlO_4]^-H^•$ site facilitate the migration of H• by converting the conventional O–H bond into a three-center O–H–O bond. This polaron conduction mechanism enables the H• to migrate more easily to adjacent BAS sites. Through multiple migrations, the unpaired electron can eventually reach a cation defect site, where it recombines with a proton to reform H•. At this stage, the hydrogen radical can be readily transferred to organic molecules adsorbed on external Al sites, thereby participating in hydrogenation reactions. This

discovery not only elucidates the stabilization mechanism of atomic hydrogen on irreducible oxides but also provides insight into the polaron-assisted migration of hydrogen across these surfaces.

### 4.2 Mechanism of sustainable hydrogen spillover

The continuity of hydrogen activation and spillover processes plays a critical role in catalytic reactions, heavily influenced by both kinetic and thermodynamic factors. A deep understanding of these processes at the atomic scale is essential for improving catalytic efficiency, as it provides insight into the driving forces behind hydrogen activation and migration.

To probe the atomic-scale dynamics of hydrogen activation, researchers have employed various theoretical approaches, Busnengo *et al.* discovered that during the dissociation of $H_2$ on the surface of $Pd_1/Cu(111)$, one hydrogen atom tends to remain bound to the active Pd site, highlighting the site-specific nature of hydrogen interactions on SAAs.[46] This finding was later supported by Lin's group, who observed a similar behavior on the $Pt_1/Cu(111)$ surface at a temperature of 300 K.[47] They identified two distinct hydrogen adsorption states at the Pd site during $H_2$ activation on $Pd_1/Cu(111)$ through XPS,[48] but the precise nature of these states remains unclear, which may influence the reactivity and sustainability of $H_2$ activation. Busnengo *et al.* employed *ab initio* molecular dynamics (AIMD) simulations to explore the $H_2$ dissociation process on $Pd_1/Cu(111)$.[46] These simulations provided detailed insights into the atomic-scale dynamics of hydrogen adsorption, dissociation, and spillover on such surfaces, complementing experimental

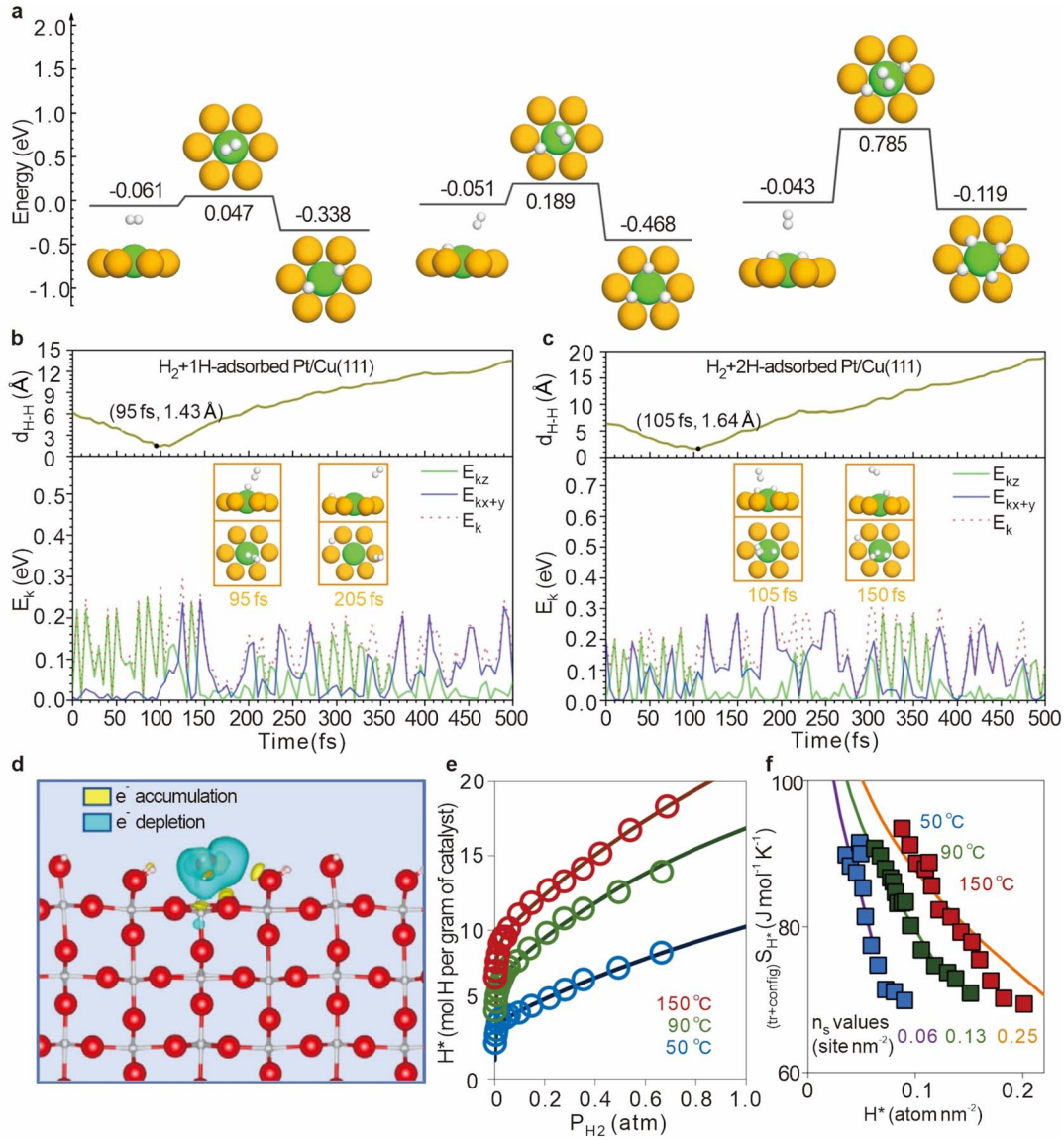


Fig. 7 (a) Energy profiles for $H_2$ dissociation on the bare-Pt/Cu(111) surface. (b) The distance between the atom closest to the spilled H atom in the $H_2$ molecule and the spilled H atom. (c) Total kinetic energy and kinetic energy components along $x + y$ and $z$. Reproduced from ref. 49. Copyright 2023 Wiley-VCH GmbH. (d) DFT calculations for H* adsorbed on fully hydroxylated rutile (110) at 0.1 H* $nm^{-2}$. (e) Temperature effects on H* adsorption. (f) Entropic contributions to hydrogen spillover energetics. Reproduced from ref. 50. Copyright 2023 Springer Nature.

findings and deepening our understanding of the catalytic behavior of SAAs. The surface structure represented by $Pt_{1-x}$/Cu(111) serves as an ideal model system for such studies (Fig. 6d). In this model, Cu atoms adjacent to Pt (referred to as $Cu_1$) and other Cu atoms (referred to as $Cu_2$) exhibit distinct coordination environments,[41] which could lead to different catalytic behaviors. As shown in Fig. 6e, substituting subsurface Cu atoms with early transition metals like vanadium has been shown to lower the diffusion barrier of H* from site 1 to site 2, thereby enhancing the efficiency of the spillover process. However, the diffusion barrier from site 2 to site 3 remains consistent across different surfaces, approximately 0.06 eV, indicating a universal characteristic of these sites in promoting hydrogen spillover.

Further investigations by Lin *et al.* revealed that the dissociation energy barrier of $H_2$ on Pt/Cu(111) surfaces increases from 0.047 eV to 0.189 eV (for 1H-hcp), and further to 0.785 eV (for 2H-hcp&fcc), indicating that the initial hydrogen adsorption can partially or completely deactivate Pt atoms (Fig. 7a).[49] To gain a better understanding of this process, they developed a neural network potential energy surface (PES) to describe the hydrogen spillover mechanism on Pt/Cu(111). Extensive molecular dynamics simulations incorporating adiabatic effects were performed, which showed that the collision between $H_2$ molecules and the pre-adsorbed H atom at the Pt site is crucial for continuous hydrogen spillover (Fig. 7b and c). At an incident kinetic energy of 0.25 eV, the horizontal kinetic energy of the $H_2$ molecule is initially too low to overcome the diffusion barrier. However, at 95 fs, the distance between the H atom in the dissociated $H_2$ and the closest H atom reaches a minimum of 1.43 Å, indicating the strongest repulsive force (Fig. 7b). This force enhances the horizontal kinetic energy of the H atom, allowing it to overcome the barrier at the Cu–Cu bridge site and spillover onto the host Cu surface. For the $H_2$ + 2H-adsorbed Pt/Cu(111) system (Fig. 7c), the strongest collision at 105 fs provides sufficient energy for the H atom to spillover onto the Cu surface, ensuring the continuity of the spillover process.

Hydrogen activation is a key step that governs the availability of active hydrogen species while hydrogen spillover plays a pivotal role in determining the quantity and distribution of these active hydrogen species across the surface of the catalyst. Recent studies by Akbar Mahdavi-Shakib *et al.* have advanced the understanding of the complex process of hydrogen spillover.[50] By investigating weakly reversible $H_2$ adsorption on Au/$TiO_2$ catalysts (Fig. 7d), the researchers quantified the surface concentration of spilled hydrogen, providing new insights into this intricate phenomenon. Their findings reveal a notably unconventional behavior: contrary to typical gas adsorption systems, where adsorption generally decreases with increasing temperature, the adsorption of H* on the Au/$TiO_2$ system exhibits a positive temperature dependence (Fig. 7e). This counterintuitive trend can be attributed to the high proton mobility on the catalyst surface, combined with configurational surface entropy, which creates favorable adsorption conditions at elevated temperatures (Fig. 7f). Additionally, the increase in temperature elevates the hydroxyl acid–base equilibrium constant on the $TiO_2$ surface, thereby increasing the number of active spillover sites. This rise in spillover points is associated with an increased concentration of zwitterions on the titanium dioxide surface, which further enhances the H* adsorption observed at higher temperatures.

### 4.3 Oxygen vacancy effects on hydrogen spillover

Metal oxides are critical components in catalytic hydrogenation reactions, and are extensively utilized in the production of both fine and bulk chemicals.[51–53] The efficiency of these reactions is heavily dependent on the ability of hydrogen atoms to diffuse across the surface of metal oxides, as this diffusion directly impacts the concentration of surface-active hydrogen species and, consequently, the overall catalytic activity.[32,54,55] However, the process of hydrogen diffusion on metal oxide surfaces is often impeded by the requirement to overcome significant energy barriers (55–236 kJ $mol^{-1}$). These barriers not only limit the rate of hydrogenation reactions but also reduce the effectiveness of the catalyst. To address this challenge, introducing oxygen vacancies into the metal oxide lattice has emerged as a potent strategy for enhancing the kinetic efficiency of hydrogen spillover. Oxygen vacancies on supports play a critical role in the spillover process not only by providing sites for the migration and stabilization of hydrogen atoms, but also by manipulating the coordination of the metal environments around them, which may directly affect the hydrogen migration barriers.[56] These vacancies not only facilitate the movement of hydrogen atoms across the catalyst surface, but also affect their stability through electron redistribution (Fig. 8).

Oxygen vacancies have a profound impact on hydrogen migration by modifying the local electronic environment. The formation of these vacancies, which involves the removal of oxygen atoms from the lattice, alters the coordination of adjacent metal atoms. It leads to a rearrangement of the local electronic structure, often resulting in an increased electron density at specific metal sites. Sun *et al.* proposed a mechanism in which oxygen vacancies create a built-in electric field (BIEF) that facilitates hydrogen spillover.[57] In their study, the Mo–Co diatomic catalyst underwent structural reconstruction in a high-temperature $H_2$ atmosphere, leading to the formation of oxygen vacancies. These vacancies caused electron accumulation near the Co atom, generating a weak BIEF between the Mo and Co atoms (Fig. 9a). Further DFT calculations confirmed that the formation of oxygen vacancies induces a differential Bader charge distribution between the Mo and Co atoms, promoting

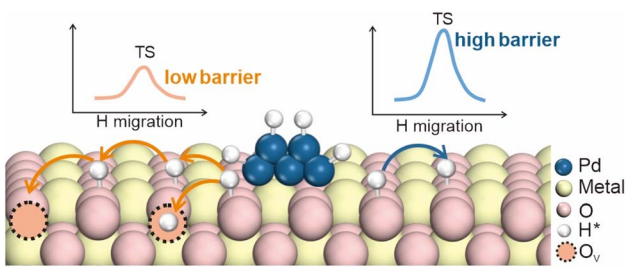


Fig. 8 Mechanism of oxygen vacancies affecting hydrogen spillover.

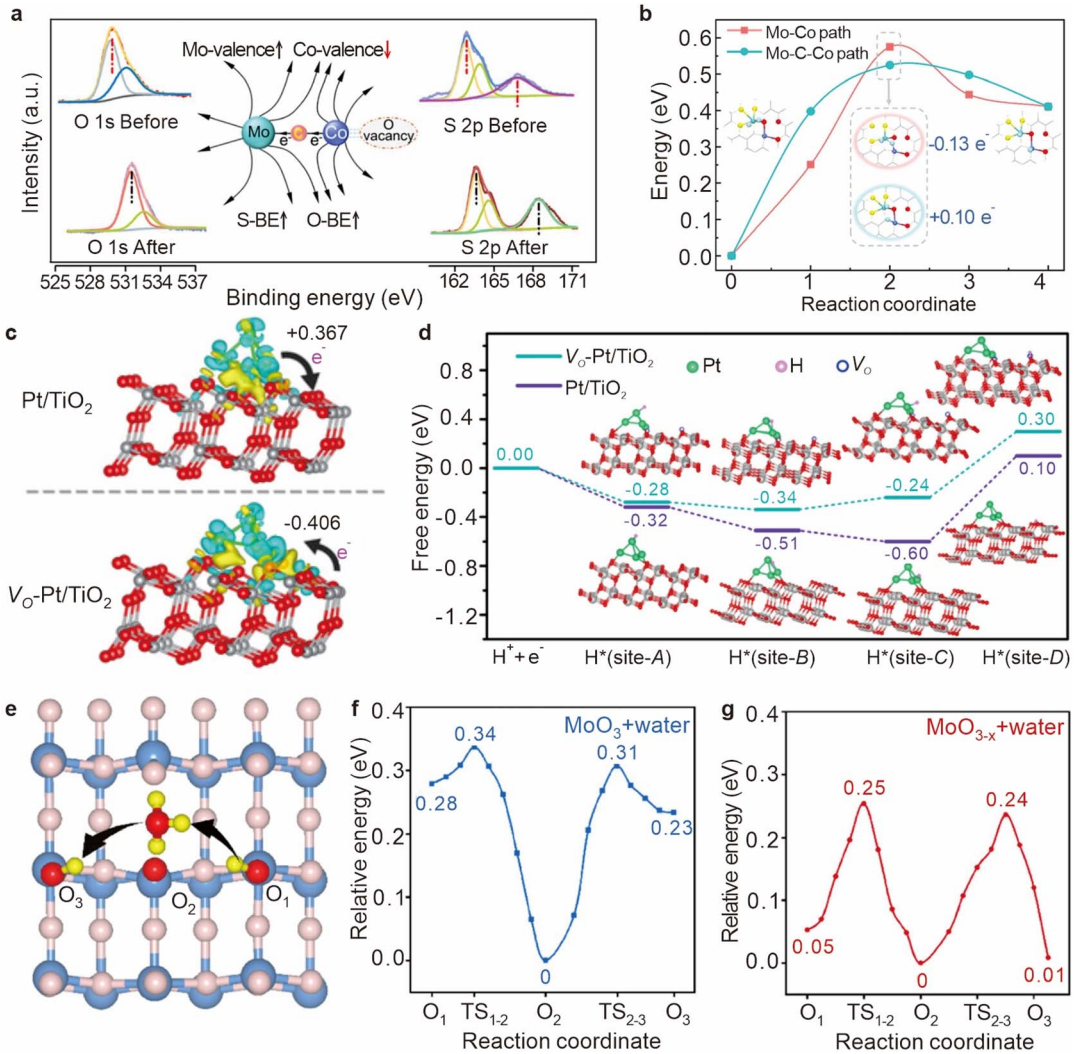


Fig. 9 (a) XPS comparison of MoCo DAC/C before and after the reaction. (b) Two alternative minimum energy paths for the first hydrogenation step of adsorbed DBT on the MoCo DACs/C surface and the corresponding structures. Reproduced from ref. 57. Copyright 2024 American Chemical Society. (c) The charge density difference analysis of $Pt/TiO_2$ and $V_O$-$Pt/TiO_2$. (d) Optimized geometric structures of Pt NCs anchored on $TiO_2$ supports with/without oxygen vacancies and the corresponding DFT calculation of the free energy. Reproduced from ref. 58. Copyright 2021 Wiley-VCH GmbH. (e) The schematic diagram of WAPH with oxygen vacancies. DFT calculations of WAPH for the (f) pristine $MoO_3$ surface and water and (g) $MoO_{3-x}$ surface and water. Reproduced from ref. 59. Copyright 2023 American Chemical Society.

the diffusion of positively charged hydrogen atoms (+0.10 $e^-$) through the localized electric field (Fig. 9b).

Oxygen vacancies also play a regulatory role in charge transfer processes between the support and the catalytically active sites, influencing hydrogen migration either positively or negatively. Pt known for its unique electronic properties and surface reactivity, is highly effective in hydrogen dissociation.[60–62] Pt's low electronegativity (2.28 compared to O's 3.44) tends to result in a higher oxidation state for Pt atoms on metal oxide supports, which can hinder hydrogen desorption. In contrast, Pt nanoclusters (NCs), which contain Pt–Pt bonds, are better at preventing electron transfer from Pt to the support, and under specific conditions, they can even reverse the direction of charge transfer. This reversal can lower the d-band center of Pt, thereby facilitating hydrogen desorption. Zheng *et al.* demonstrated that oxygen vacancies in the support material can induce unique dual effects of electron-rich Pt in $Pt/TiO_2$ catalysts, including reverse charge transfer and enhanced hydrogen spillover.[58] In a $Pt/TiO_2$ system, approximately 0.367 electrons are transferred from Pt nanoclusters to $TiO_2$, but in a $V_O$-$Pt/TiO_2$ system, about 0.406 electrons are transferred from $TiO_2$ to Pt nanoclusters, indicating that oxygen vacancies can reverse the charge transfer direction, enriching the Pt nanoclusters with electrons (Fig. 9c). Further free energy calculations revealed significant differences in the hydrogen adsorption free energy ($\Delta G_H$) at different sites on the $Pt/TiO_2$ surface, with a variance of up to 0.70 eV between site-C and site-D (Fig. 9d). In contrast, the $\Delta G_H$ difference between the two sites on $V_O$-$Pt/TiO_2$ was reduced to 0.54 eV, suggesting that oxygen vacancies substantially enhance the hydrogen spillover effect.

The role of acidic hydroxyl groups on the surface of oxides, or defect sites introduced during synthesis, is well-documented in

promoting hydrogen transfer processes.[9,63,64] Recent studies have highlighted the significance of these groups in facilitating the migration of hydrogen atoms, especially when synergized with other molecules or structural features of the catalyst. Wang *et al.* demonstrated that gaseous organic molecules containing carbonyl functional groups could facilitate the migration of hydrogen from Pt to Fe sites on an oxide surface.[65] This mechanism is reminiscent of molecular coenzymes in enzymatic reactions, where the coenzyme assists in the transfer of reactive groups between sites, thereby enhancing the overall catalytic process.[66] Metal–organic frameworks (MOFs) have also been recognized for their ability to absorb water through their clusters or ligands.[67,68] Gu *et al.* emphasized this understanding by constructing a water-assisted spillover pathway in a Pt@MOF-801 system.[69] Their calculations revealed that the energy barrier for hydrogen migration *via* this water-assisted pathway is lower than that of the traditional ligand-based spillover route, underscoring the potential of water molecules in facilitating hydrogen diffusion.

On the surface of metal oxides, the presence of water can further enhance the diffusion of hydrogen atoms through a mechanism known as proton-coupled electron transfer (PCET). This process, also referred to as the water-assisted proton jump (WAPH),[70,71] involves the temporary formation of hydronium ions ($H_3O^+$) as water molecules absorb hydrogen atoms. The electrons from these hydrogen atoms are then transferred to the d-orbitals of the metal oxide, promoting subsequent hydrogenation reactions on metal oxide-supported catalysts.[72,73] Wang *et al.* showed that the presence of oxygen vacancies can accelerate the adsorption of water molecules (Fig. 9e),[59] thereby reducing the energy barrier associated with WAPH. Their findings indicate that on a defect-free surface, the barrier energy for proton jumping is approximately 0.30 eV (Fig. 9f), but this barrier decreases to 0.25 eV when oxygen vacancies are present (Fig. 9g). The impact of oxygen vacancies on proton jumping is further elucidated by charge density distribution studies, which reveal how these vacancies alter the electronic states of surrounding atoms, particularly oxygen and neighboring metal atoms.

# 5. Hydrogenations by spillover

## 5.1 Hydrogenation by spillover mechanism

The hydrogenation process involves two key steps: the formation of adsorbed H* on a catalyst's surface and the subsequent desorption of these species to drive the hydrogenation reaction.[74,75] Traditionally, these steps are managed by a single catalytic component, but it often leads to a balance in optimizing both formation and desorption. To overcome this limitation, researchers have used hydrogen spillover which decouples these steps by employing distinct catalytic components specialized for each function.[76,77]

Following the hydrogen spillover, the active hydrogen atoms which have migrated to the support surface may participate in subsequent catalytic reactions under mild conditions depending on the properties of supports. These hydrogen atoms interact with reactant molecules, particularly in systems where the support material, such as metal oxides, provides active sites like oxygen vacancies. These sites not only stabilize the hydrogen atoms but also facilitate the activation and adsorption of reactants. The spillover process effectively increases the availability of hydrogen atoms on the support surface, which can significantly enhance the overall reaction rate and improve the efficiency of the hydrogenation process.[12,78] Such a separation strategy not only maximizes the overall efficiency of hydrogen utilization but also significantly enhances the selectivity and precision of the hydrogenation process, leading to improved catalytic performance.

**5.1.1 Improved hydrogenation reactivity by hydrogen spillover.** Achieving effective hydrogenation at low temperatures has been a long-standing challenge in catalytic chemistry due to the inherent high binding energy of metal surfaces, which can impede catalytic activity. The hydrogen spillover pairs metals with different binding strengths to optimize the reaction dynamics. A prime example of this strategy's success is the work by Zhang *et al.*, which synthesized a PtCo alloy supported on $CoBO_x$.[79] As shown in Fig. 10c, this innovative catalyst system demonstrated an extraordinary turnover frequency (TOF) of 2479 $h^{-1}$ in the hydrogenation of cinnamaldehyde (CAL), a performance that was unattainable using $CoBO_x$ alone due to its lack of catalytic activity in the absence of the PtCo alloy.[11,80] The remarkable catalytic efficiency observed in this system is attributed to the synergistic interaction between the PtCo alloy and the $CoBO_x$ support. The alloy effectively facilitates the adsorption and activation of hydrogen, while the $CoBO_x$ support promotes the desorption of hydrogen, ensuring a continuous and efficient hydrogenation process.

Electrochemical dechlorination is of critical importance for the environmental remediation of organochlorine compounds, which are notorious for their "teratogenic, carcinogenic, and mutagenic" properties, posing severe risks to both ecosystems and human health. An exemplary advancement in this field is the CoPc/CNT catalyst developed by Wang *et al.*, which demonstrated the efficient conversion of dichloroacetic acid (DCA) into ethylene and chloride ions in aqueous solutions.[83]

For effective electrochemical dechlorination, it is essential to optimize the dissociation of water molecules into reactive H*, while concurrently inhibiting the undesirable recombination of H* into $H_2$. This balance is crucial because, while noble metal electrodes are highly effective at promoting water dissociation,[84] they also tend to enhance the recombination of H*, thereby reducing its availability for dechlorination reactions.[85,86] Consequently, there is a pressing need to develop innovative electrode materials that can efficiently promote water dissociation while minimizing H* recombination to maximize dechlorination efficiency. To address the challenge of optimizing the generation, transfer, and utilization of atomic hydrogen in electrochemical processes, Zhang *et al.* developed an innovative electrocatalytic system based on a reverse hydrogen spillover effect,[81] using a $Co_1$–$TiO_x$/Ti electrode. Individual cobalt atoms are anchored onto a titanium oxide substrate, leveraging the excellent hydrolytic ionization and hydrogen adsorption properties of the $TiO_x$ support. This configuration allows for the rapid migration of hydrogen atoms

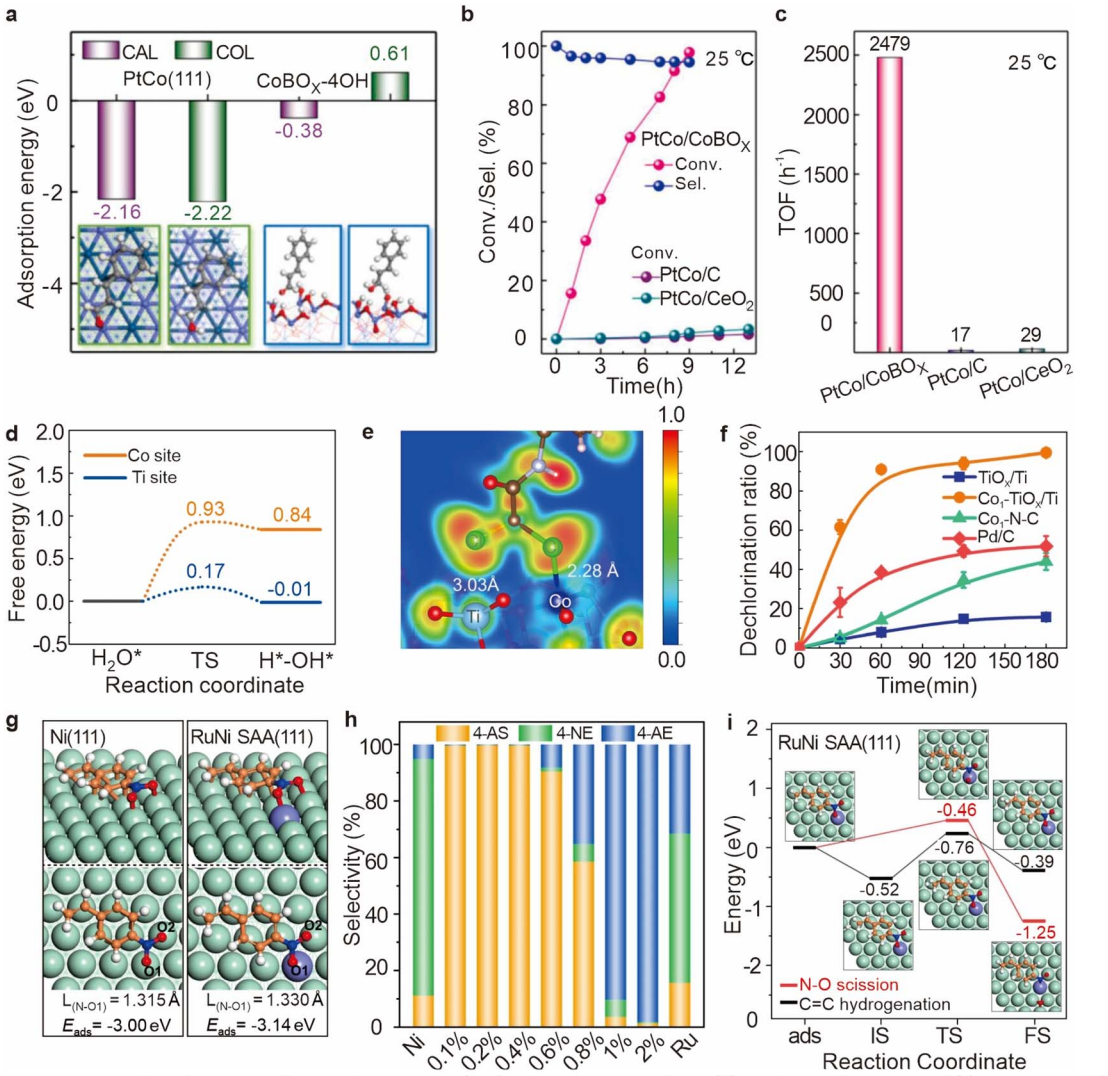


Fig. 10 (a) Adsorption energies and configurations of CAL and COL on PtCo(111) and CoBO$_x$-6OH surfaces. (b) Catalytic performance and (c) TOF values of the CAL hydrogenation. Reproduced from ref. 79. Copyright 2021 Elsevier. (d) Energy barrier for water dissociation on Co$_1$–TiO$_x$/Ti. (e) ELF analysis of CAP adsorption on Co$_1$–TiO$_x$/Ti. (f) Dechlorination ratio on Co$_1$–TiO$_x$/Ti and other control samples. Reproduced from ref. 81. Copyright 2024 Wiley-VCH GmbH. (g) Adsorption configurations of 4-NS on Ni(111) and RuNi SAA(111) surfaces. (h) Product distribution in the presence of monometallic Ni, Ru, and RuNi catalysts with various Ru loadings (0.1–2 wt%). (i) Potential energy profiles and the corresponding optimized structures for C=C hydrogenation and N–O scission in 4-NS over the RuNi SAA(111) surface. Reproduced from ref. 82. Copyright 2022 Springer Nature.

to the cobalt sites, where they actively participate in the dechlorination reaction *via* the reverse hydrogen spillover mechanism (Fig. 10d and e). The electrochemical performance of the Co$_1$–TiO$_x$/Ti electrode was rigorously evaluated, demonstrating a markedly higher dechlorination efficiency (99%) compared to the TiO$_x$/Ti electrode alone (Fig. 10f). These findings highlight the potential of hydrogen spillover systems for advancing the effectiveness of catalytic processes, particularly in applications requiring precise control over hydrogen atom dynamics.

**5.1.2 Improved hydrogenation selectivity by hydrogen spillover.** In heterogeneous catalysis, the presence of multiple catalytic sites with varying coordination environments and electronic structures often leads to diverse adsorption modes for reaction intermediates, resulting in poor selectivity. This issue is particularly evident in reactions like the semi-hydrogenation of acetylene on palladium surfaces, where different configurations of palladium atoms lead to distinct adsorption behaviors. On palladium surfaces, acetylene can adsorb in three primary modes: the acetylene mode and two sigma modes on continuous palladium active sites, and the π-bond mode on isolated palladium single atoms.[87] The acetylene and sigma modes exhibit strong adsorption, which can lead to the undesired dimerization of acetylene or its over-hydrogenation to ethane. In contrast, the π-bond mode, which is associated with weaker adsorption, promotes the desorption of ethylene from the palladium surface, thereby preventing further hydrogenation to ethane.[88,89]

The activated adsorption of specific functional groups is a crucial step in the selective hydrogenation of substrates, as it directly influences both the efficiency of catalytic reactions and the selectivity of the resulting products. While an increase in catalytic activity can sometimes lead to a decrease in the selectivity of the target product,[90–92] the PtCo/$CoBO_x$ catalyst demonstrates a remarkable exception, maintaining a selectivity of 94.5% (Fig. 10b). Through DFT calculations, Zhang *et al.* discovered that this high selectivity is due to the interaction between the carbonyl group (–C=O) and three surface hydroxyl groups on the catalyst.[81] This interaction causes CAL to adopt an inclined adsorption configuration on the catalyst surface, which positions the C=C bond away from the surface while elongating the C=O bond. Furthermore, the adsorption energy of the corresponding alcohol product on the $CoBO_x$-6OH surface is +0.61 eV, indicating that desorption is energetically favorable (Fig. 10a).

In catalyst design, researchers must carefully consider surface properties to achieve the activated adsorption of specific functional groups. This may involve fine-tuning the composition, structure, and surface modifications of the catalyst to optimize its ability to adsorb and transform particular substrates. Liu *et al.* reported a RuNi single-atom alloy catalyst where hydrogen dissociates at an adjacent Ni site and then undergoes hydrogenation at the $Ru^{\delta-}$ site (Fig. 10g).[82] This catalyst demonstrated excellent performance in the selective hydrogenation of 4-nitrostyrene to produce 4-aminostyrene (Fig. 10h). *In situ* experimental studies, supported by DFT calculations (Fig. 10i), revealed that the Ru–Ni interface site, as the characteristic active center, facilitated the activation and adsorption of the nitro group with a lower energy barrier (0.46 eV) compared to the monometallic Ni catalyst (0.74 eV), ultimately leading to the successful production of the target compound.

### 5.2 Oxygen vacancy effects on hydrogenation by spillover

Although the concept of hydrogenation by spillover has been recognized in the field of catalytic hydrogenation for many years, the precise structural characteristics of the support required to facilitate effective hydrogen spillover remain inadequately understood.[9–13] The efficiency of hydrogenation by spillover is not solely dependent on the catalyst's structural properties, but the reactant's functional groups and substituents also determine its affinity for the catalyst surface and its susceptibility to hydrogenation. Additionally, the nature of the active hydrogen species and the presence of promoters or dopants on the catalyst can further modify these interactions, ultimately affecting the overall catalytic performance.

**5.2.1 Oxygen vacancy effects on hydrogenation reactivity.** Oxygen vacancies enhance hydrogenation activity by creating a local charge imbalance that alters the adsorption properties of the metal oxide surface.[93] As a common type of point defect in metal oxides, oxygen vacancies significantly influence electron transfer within reducible metal oxide supports, thereby providing more adsorption sites or more efficient catalytically active sites.[94–97] Xie *et al.* demonstrated that oxygen vacancies in the $ZnO_{1-x}$/Cu catalyst not only enhance the activation of $CO_2$ but also improve the yield of methanol.[98] The specific properties of oxygen vacancies (concentration, type, and coordination) play a crucial role in determining the overall effectiveness of

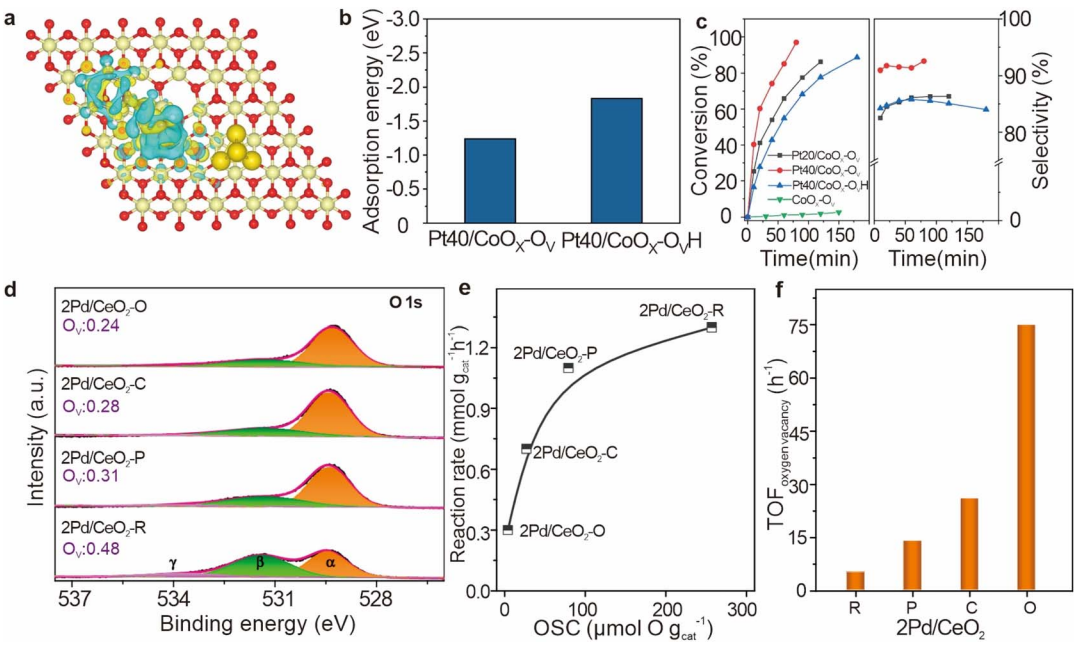


Fig. 11 (a) The charge density differences of a CALD molecule adsorbed on Pt40/$CoO_x$–$O_V$H catalysts. (b) Adsorption energies of CALD on Pt40/$CoO_x$–$O_V$ and Pt40/$CoO_x$–$O_V$H catalysts. (c) Catalytic performance of different catalysts. Reproduced from ref. 100. Copyright 2024 Elsevier. (d) *In situ* XPS curves of O 1s for the reduced Pd/$CeO_2$ catalysts. (e) Reaction rate as a function of the number of surface oxygen vacancies (OSCs). (f) $TOF_{oxygen\ vacancy}$ over various Pd/$CeO_2$ catalysts. Reproduced from ref. 23. Copyright 2020 American Chemical Society.

catalysts. Xiang *et al.* reported that a $CeFeO_x$–Au catalyst with a controllable concentration of oxygen vacancies significantly enhances catalytic activity and selectivity in CO oxidation due to the modified surface electronic properties and improved interaction between oxygen vacancies and Au single atoms.[99] Xu *et al.* highlighted that different oxygen vacancy configurations can greatly affect hydrogenation performance.[100] Their findings showed that the Pt40/$CoO_x$–$O_V$H catalyst had a lower selectivity for cinnamyl alcohol (CALA) compared to Pt40/$CoO_x$–$O_V$ (Fig. 11c). Computational and charge density analyses revealed that the stronger binding and increased charge transfer between cinnamaldehyde (CALD) and Pt40/$CoO_x$–$O_V$H likely lead to preferential hydrogenation of the C=C bond, reducing selectivity for CALA (Fig. 11a and b).

In the context of hydrogenation reactions, the density of oxygen vacancies on catalyst surfaces plays a crucial role in determining catalytic activity. Liu *et al.* confirmed a strong correlation between the formation energy of oxygen vacancies and the hydrogenation performance of $CO_2$.[23] For Pd/$CeO_2$ catalysts with different morphologies (Fig. 11d), the oxygen vacancy density follows the order: 2Pd/$CeO_2$–R (0.48) > 2Pd/$CeO_2$–P (0.31) > 2Pd/$CeO_2$–C (0.28) > 2Pd/$CeO_2$–O (0.24), as indicated by O 1s spectra and supported by Ce 3d spectral analysis. As the oxygen storage capacity (OSC) increases, the rate of $CO_2$ adsorption and activation on the oxygen vacancies also increases, resulting in higher reaction rates. However, this increase becomes less pronounced at higher OSC values, showing diminishing returns at elevated oxygen vacancy concentrations (Fig. 11e). To further assess the intrinsic activity of oxygen vacancies, the turnover frequency for oxygen vacancy-related reactions was calculated. The 2Pd/$CeO_2$–R catalyst, which exposes the (110) and (111) crystal facets, exhibits the lowest TOF, whereas 2Pd/$CeO_2$–O, which exposes the (111) facet, demonstrates the highest TOF (Fig. 11f). These findings suggest that the formation and reactivity of oxygen vacancies are influenced by both the crystal structure and the ease with which vacancies form. On $CeO_2$–R, the formation of oxygen vacancies is facilitated by the high oxygen mobility and low vacancy formation energy of the $CeO_2$(110) facet, but this leads to lower reactivity. In contrast, $CeO_2$–O, with a lower density of oxygen vacancies and a higher energy barrier for vacancy formation on the (111) facet, shows stronger interaction with $CO_2$ and higher reactivity for hydrogenation. This difference in reactivity can be explained by the balance between vacancy formation and filling.

**5.2.2 Oxygen vacancy effects on hydrogenation selectivity.** Oxygen vacancies can also influence hydrogenation selectivity by altering the adsorption configuration of reactant molecules. Reactants containing oxygen-functional groups, such as carbonyl or hydroxyl groups, may preferentially adsorb to these vacancies. This specific adsorption configuration can either promote or hinder certain reaction pathways, allowing the catalyst to selectively favor the formation of specific hydrogenation products (Fig. 12a).[101,102] For instance, in lignin hydrodeoxygenation, transition metal oxide catalysts with engineered oxygen vacancies exhibit improved selectivity due to modified reactant binding configurations.[103] The presence of oxygen vacancies in $BiVO_4$ and $TiO_x$ catalysts significantly impacts product selectivity during water oxidation and fatty acid deoxygenation, respectively, by modulating the electronic structure and stabilizing reaction intermediates.[104,105] Wang *et al.* reported that at the copper–cerium interface, oxygen vacancies induce a downward-oriented adsorption configuration (D-configuration) of the hydroxyl group.[106] This configuration exhibits a higher adsorption energy (−1.85 eV) compared to the upward-oriented configuration (U-configuration), as depicted in Fig. 12b. Additionally, the bond length of the C=O group in the glycol molecule increases in the D-configuration (Fig. 12c), and there is a notable difference in hydride transfer barriers between the D- and U-configurations (Fig. 12d), which can be attributed to minor geometric reconstructions of the copper surface during hydrogen transfer. These observations underscore the critical influence of oxygen vacancies on the adsorption structures, which in turn play a vital role in modulating the subsequent hydrogenation processes.

Additionally, in the selective hydrogenation of butenal, metal-free $CeO_2$ nanorods with a high concentration of surface oxygen vacancies exhibit superior selectivity for C=O hydrogenation compared to C=C hydrogenation, achieving turnover frequencies comparable to those of precious metal-based catalysts, along with very high selectivity for butanol. This enhanced selectivity is attributed to the interaction between the oxygen vacancies and the C=O group, which stabilizes the group and promotes its preferential hydrogenation.[28] Similarly, another study on selective hydrogenation of α,β-unsaturated hydrocarbons using transition metal photocatalysts supported by LDH (layered double hydroxide) surfaces found that oxygen vacancies act as active adsorption centers, favoring the adsorption of C=O groups while hindering the adsorption of C=C groups. This selective adsorption pathway ensures high cinnamyl alcohol yield.[108]

The importance of oxygen vacancies extends beyond simple reactant adsorption and is particularly relevant in the selective hydrogenation of functionalized nitroaromatics. The selective reduction of nitro groups to amines is a key reaction in the synthesis of various fine chemicals, pharmaceuticals, and agrochemicals; the adsorption configuration of the nitro group at an oxygen vacancy is highly sensitive to the presence and properties of adjacent substituents on the aromatic ring.[109–115] *Ortho*-substituents that are positioned near the nitro group can exert both electronic and spatial effects that influence the interaction between the nitro group and the catalyst surface (Fig. 12e).[107] When the *ortho*-position on the benzene ring is occupied by a larger substituent, steric effects can weaken the adsorption of the reactant molecule at the oxygen vacancy, thereby reducing catalytic activity. Under identical reaction conditions, the hydrogenation rate of 4-nitrotoluene by PdHD/$WO_3$-350 is observed to be 19 times greater than that of 2-nitrotoluene (Fig. 12f). This significant difference in catalytic activity highlights the impact of steric effects, where the presence of an *ortho*-methyl group at the oxygen vacancy significantly diminishes the efficiency of *p*-nitro-hydrogenation.

Oxygen vacancies promote catalytic hydrogenation primarily by regulating the electronic structure and surface properties of

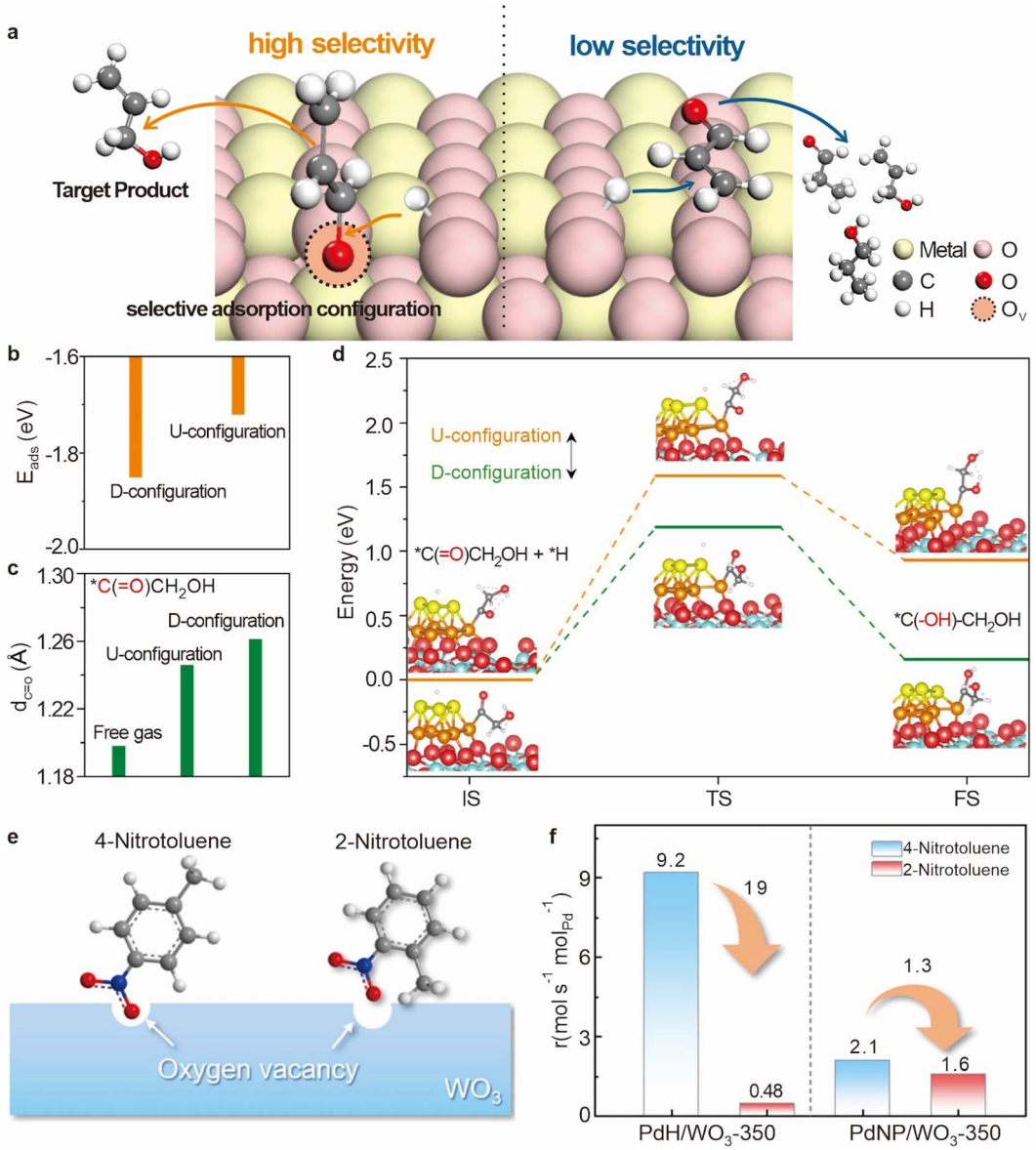


Fig. 12 (a) Diagram of oxygen vacancies affecting hydrogenation by spillover. (b) Comparison of $E_{ads}$ in two configurations. (c) Change in the distance of C=O compared to the free gas. (d) Kinetic barrier diagram for glycolyl hydrogenation *via* the D- and U-configurations. Reproduced from ref. 106. Copyright 2024 American Chemical Society. (e) Scheme of the adsorption configuration of 2-nitrotoluene and 4-nitrotoluene on the oxygen vacancy of $WO_3$. (f) Reaction rate of 2-nitrotoluene/4-nitrotoluene hydrogenation by using the PdHD/$WO_3$-350 and PdNP/$WO_3$-350 catalysts. Reproduced from ref. 107. Copyright 2023 American Chemical Society.

the catalyst. Ongoing research will continue to explore the mechanisms by which oxygen vacancies influence different catalytic systems and how these active sites can be optimized through material design to achieve more efficient and environmentally friendly catalytic processes.

### 5.3 Other effects on hydrogenation by spillover

In the study of hydrogenation by spillover reactions, introducing lattice defects in the support material can lead to additional active sites or alter the charge distribution to optimize catalytic performance. Additionally, controlling the morphology, regulating the crystal surface, and modifying the catalyst surface can provide more favorable adsorption geometries and reduce activation barriers, thereby promoting catalytic reactions. For instance, selectively exposing specific crystal faces can change the density and distribution of active sites on the catalyst.[116] Jiang *et al.* dispersed Pd atoms onto Cu nanomaterials with distinct crystallographic surfaces.[117] Three types of potential catalytic sites were identified: Pd-related sites, interfacial Cu sites, and Cu sites (Fig. 13a and b). Both $Pd_1$/Cu catalysts demonstrated excellent catalytic performance and high durability during the semi-hydrogenation of phenylacetylene to styrene (PhCH=$CH_2$) under mild conditions (Fig. 13c). Theoretical calculations revealed that hydrogenation on Cu using spilled hydrogen atoms is highly dependent on the

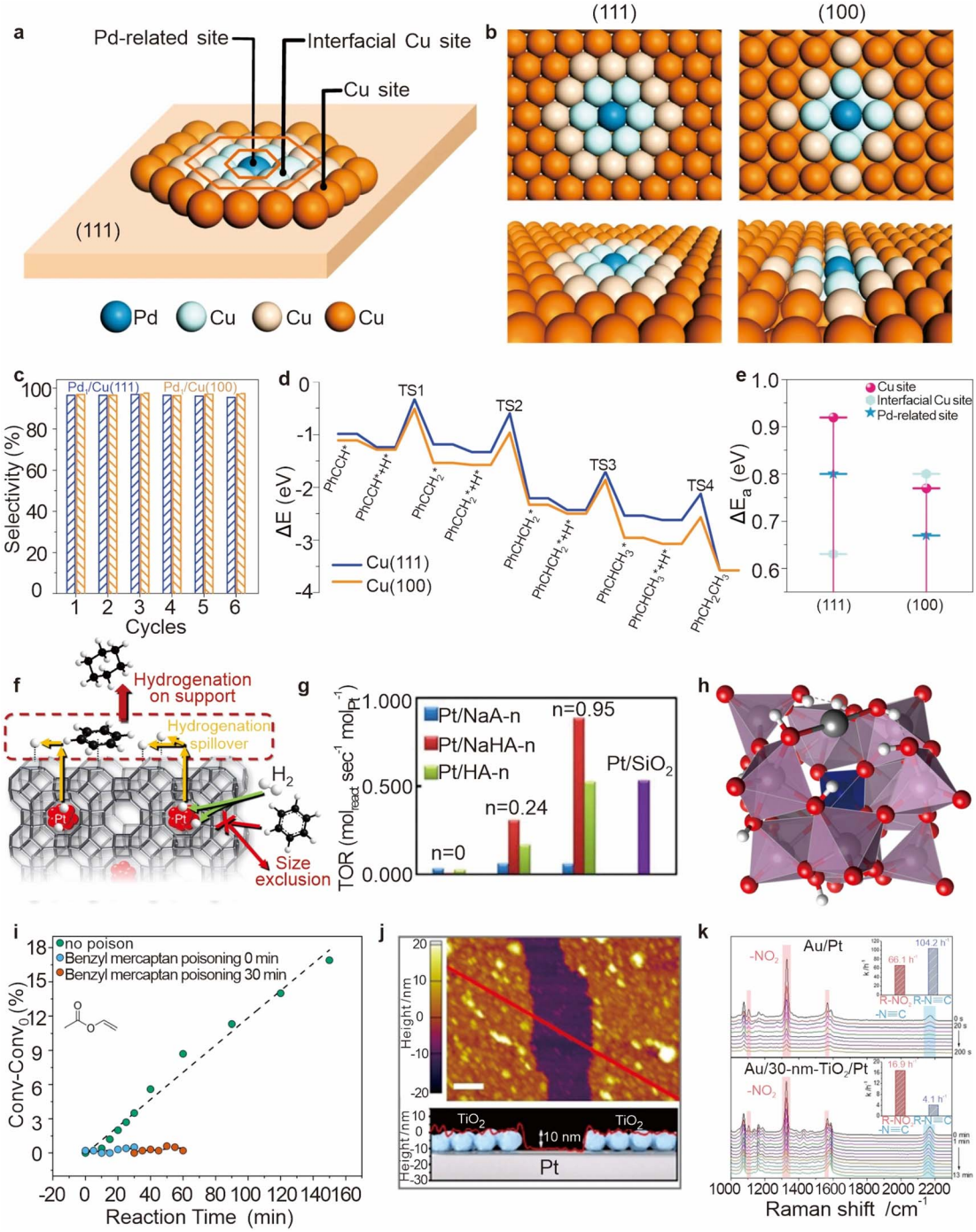


Fig. 13 (a) Three kinds of possible reactive sites on the $Pd_1/Cu$ surface. (b) Top and side views of the $Pd_1/Cu(111)$ and $Pd_1/Cu(100)$ surface models. (c) Catalytic durability of $Pd_1/Cu(111)$ and $Pd_1/Cu(100)$ in the semi-hydrogenation of PhC≡CH. (d) Calculated barriers for stepwise hydrogenation of PhC≡CH on the two low-Miller-index Cu surfaces. (e) Calculated barriers for TS1 over different active sites on different $Pd_1/Cu$ catalysts. Reproduced from ref. 117. Copyright 2020 Springer Nature. (f) Pt encapsulated in a dense support matrix that allows selective diffusion of hydrogen over organic reactants. (g) Turnover rates in benzene hydrogenation. Reproduced from ref. 9. Copyright 2014 Springer Nature. (h) Structure of $PMo11O39Pd_1$-H16. (i) Reaction kinetics for the hydrogenation of VA with the addition of 2 equivalents benzyl mercaptan after different reaction times. Reproduced from ref. 118. Copyright 2022 Wiley-VCH GmbH. (j) AFM image of the $TiO_2$ nanoparticle monolayer assembled on a smooth Pt film ($TiO_2$/Pt). (k) *In situ* SERS spectra of the selective hydrogenation of R–$NO_2$ in the presence of R–N≡C on Au/Pt and Au/30 nm-$TiO_2$/Pt, respectively. Reproduced from ref. 53. Copyright 2020 Wiley-VCH GmbH.

specific surface structure of copper. The Cu(100) plane exhibited a lower hydrogenation barrier and higher surface coverage of phenylacetylene (PA) compared to the Cu(111) plane, facilitating PA conversion on Cu(100) (Fig. 13d). This enhanced catalytic activity on Cu(100) is attributed to more effective rehybridization of the s–p–d orbitals, leading to greater

stabilization of the transition state (TS1). The energy barrier for TS1 at the Cu site of $Pd_1$/Cu(111) is significantly higher than at the Pd site or the Cu site at the interface (Fig. 13e). The superior catalytic activity of Cu(100) compared to Cu(111) underscores its potential as an effective support material for enhancing catalytic performance.

The influence of the support's particle size is equally important, as it directly impacts the specific surface area and the number of active sites. A study by Juhwan Im *et al.* demonstrated that increasing the surface area of an aluminosilicate matrix significantly enhances catalytic activity for benzene hydrogenation.[9] The Pt/NaHA-0.95 sample, characterized by a large surface area and a highly amorphous structure, exhibited the highest catalytic activity, surpassing even Pt/$SiO_2$ samples with larger accessible metal surface areas (Fig. 13f and g). With careful catalyst nanostructure design, it is possible to achieve high hydrogenation and dehydrogenation catalytic activity. This principle was further confirmed by Wei *et al.*, who enhanced the selectivity of hydrogen spillover by carefully controlling the chemical potential of H*.[53] They found that as H* spilled over from $TiO_2$, the coverage of active hydrogen at the Au site decreased with increasing spillover distance due to the presence of a reaction barrier (Fig. 13j), thereby reducing the chemical potential of active hydrogen. As the chemical potential decreases, the available hydrogen preferentially follows hydrogenation pathways that require lower energy, thus enhancing selectivity (Fig. 13k). This work provides valuable molecular-level insights into the mechanism of hydrogen activation, offering a deeper understanding of the rational design of selective hydrogenation catalysts.

While the hypothesis that spillover H* directly contributes to hydrogenation reactions has been proposed, it is important to note that for certain reactants requiring direct H transfer from the metal active site, spillover H* may not participate in the hydrogenation process.[12,119] In the structure of $PMo_{11}O_{39}Pd_1$-$H_{16}$ (Fig. 13h), the introduction of Pd poison (benzyl mercaptan) prevents the conversion of vinyl acetate, which contains C=C bonds, causing the reaction rate to drop to zero (Fig. 13i). This indicates that the hydrogen involved in the hydrogenation of the C=C bond originates directly from the Pd active site, rather than from spilled H*.[118]

## 6. Conclusions and perspective

Enhancing the efficiency of active sites has long been a significant challenge for supported catalysts, and the spillover effects offer a promising strategy to activate more sites on the supports. The advent of advanced surface characterization techniques such as *in situ* spectroscopy and high-resolution electron microscopy has enabled researchers to observe the dissociation of $H_2$ on active metal sites, thereby providing direct and compelling evidence of the spillover phenomenon. The integration of machine learning with DFT calculations has illuminated the underlying mechanisms of hydrogen spillover. The hydrogenation efficiency of spilled hydrogen can be significantly enhanced by manipulating various factors, including the introduction of oxygen vacancies, the modification of metal crystal surfaces, and so on. Recent studies provide compelling evidence of the catalytic functions of hydrogen spillover, highlighting its potential in the design and development of advanced catalysts. The support effects especially the effects of the oxygen vacancies on hydrogen dissociation, hydrogen spillover, and the hydrogenation process are introduced in detail.

The hydrogen dissociation process is sometimes the rate-limiting step in hydrogenation reactions. The dissociation mode of hydrogen significantly influences the type and behavior of active hydrogen species, which in turn dictates the catalytic reaction pathway and product distribution. Recent studies have shown that by carefully designing and engineering the catalyst's structure, the presence of oxygen vacancies on the CoO(100)–$O_V$ surface made the adsorption and dissociation process of $H_2$ more favorable. In the hydrogen spillover process, oxygen vacancies have a profound impact on hydrogen migration by modifying the local electronic environment. The formation of these vacancies, which involves the removal of oxygen atoms from the lattice, alters the coordination of adjacent metal atoms. It leads to a rearrangement of the local electronic structure, resulting in an increased electron density at specific metal sites. In the hydrogenation process, oxygen vacancies enhance hydrogenation activity by creating a local charge imbalance that alters the adsorption properties of the metal oxide surface. These vacancies create stronger and more selective binding sites, which profoundly influence the orientation and reactivity of the adsorbed species.

Although significant progress has been made in hydrogen spillover and its application to hydrogenation, several challenges remain for practical implementation. First, developing accurate imaging and characterization techniques: the characterization of active sites is still a challenge for the reaction process. It is difficult to separate the hydrogenation reactions occurring on the metal catalyst from those on the support to accurately assess the spillover efficiency of active hydrogen species on the support. Secondly, developing experimental methods: catalysts with oxygen vacancies are usually not stable, and thus how to equilibrate the stability and reactivity of materials is still a challenge. Finally, developing theoretical calculations with machine learning methods: the combination of dynamics and thermodynamics is necessary to be considered for the migration rate of spillover species, which is essential for understanding the impact of spillover on enhancing hydrogenation activity. The influence of oxygen vacancies in supports on the hydrogenation reaction varies depending on their location. A deeper understanding of oxygen vacancy migration behavior can inform the design of novel catalyst systems for highly selective chemical reactions. Therefore, a broader investigation of the dynamic activities of species behaviors on various types of supports, by *ab initio* molecular dynamics, machine learning, and other more accurate methods, is strongly recommended. In summary, the spillover effect plays a crucial role in enhancing catalytic performance, offering a pathway to more efficient and selective hydrogenation processes. The deep understating of support effects especially oxygen vacancy effects presents significant opportunities and

challenges for chemical synthesis, energy storage, and conversion technologies, requiring a multidisciplinary approach that combines experimental insights with advanced computational techniques.

## Data availability

No primary research results, software or code have been included and no new data were generated or analysed as part of this review.

## Author contributions

Lijuan Xie: conceptualization; resources; writing – original draft; writing – review & editing. Jinshan Liang: resources; writing – review & editing. Lizhi Jiang: conceptualization; funding acquisition; supervision; writing – review & editing. Wei Huang: supervision; project administration. All authors have given approval to the final version of the manuscript.

## Conflicts of interest

The authors declare no conflict of interest.

## Acknowledgements

The authors would like to acknowledge the financial support from the National Natural Science Foundation of China (Grant No. 22102027), Fujian Province Natural Science Foundation of China (Grant No. 2022J01653), and start-up research funding of Fujian Normal University (Grant No. Y0720309K13).

## References

1 Y. Y. Geng and H. Li, Hydrogen spillover-enhanced heterogeneously catalyzed hydrodeoxygenation for biomass upgrading, *ChemSusChem*, 2022, **15**, e202102495.
2 J. Li, H. Liu, W. Gou, M. Zhang, Z. Xia, S. Zhang, C. Chang, Y. Ma and Y. Qu, Ethylene-glycol ligand environment facilitates highly efficient hydrogen evolution of Pt/CoP through proton concentration and hydrogen spillover, *Energy Environ. Sci.*, 2019, **12**, 2298–2304.
3 J. Cho, M. Kim, H. Seok, G. H. Choi, S. S. Yoo, N. C. Sagaya Selvam, P. J. Yoo and T. Kim, Patchwork-structured heterointerface of 1T-WS2/a-$WO_3$ with sustained hydrogen spillover as a highly efficient hydrogen evolution reaction electrocatalyst, *ACS Appl. Mater. Interfaces*, 2022, **14**, 24008–24019.
4 F. Cao, Y. Xiao, Z. Zhang, J. Li, Z. Xia, X. Hu, Y. Ma and Y. Qu, Influence of oxygen vacancies of $CeO_2$ on reverse water gas shift reaction, *J. Catal.*, 2022, **414**, 25–32.
5 J. Song, Z. Huang, L. Pan, J.-J. Zou, X. Zhang and L. Wang, Oxygen-deficient tungsten oxide as versatile and efficient hydrogenation catalyst, *ACS Catal.*, 2015, **5**, 6594–6599.
6 N. Zhao, J. Li, X. Chang, W. Zheng, J. Zhang and X. Liu, Synthesis and application of graphdiyne-based materials for advanced chemical sensors, *Coord. Chem. Rev.*, 2024, **521**, 216171.
7 J. Li, J. Hu, M. Zhang, W. Gou, S. Zhang, Z. Chen, Y. Qu and Y. Ma, A fundamental viewpoint on the hydrogen spillover phenomenon of electrocatalytic hydrogen evolution, *Nat. Commun.*, 2021, **12**, 3502.
8 L. Wang and R. T. Yang, New sorbents for hydrogen storage by hydrogen spillover – a review, *Energy Environ. Sci.*, 2008, **1**, 268–279.
9 J. Im, H. Shin, H. Jang, H. Kim and M. Choi, Maximizing the catalytic function of hydrogen spillover in platinum-encapsulated aluminosilicates with controlled nanostructures, *Nat. Commun.*, 2014, **5**, 3370.
10 W. Karim, C. Spreafico, A. Kleibert, J. Gobrecht, J. VandeVondele, Y. Ekinci and J. A. van Bokhoven, Catalyst support effects on hydrogen spillover, *Nature*, 2017, **541**, 68–71.
11 G. Kyriakou, M. B. Boucher, A. D. Jewell, E. A. Lewis, T. J. Lawton, A. E. Baber, H. L. Tierney, M. Flytzani-Stephanopoulos and E. C. H. Sykes, Isolated metal atom geometries as a strategy for selective heterogeneous hydrogenations, *Science*, 2012, **335**, 1209–1212.
12 R. Prins, Hydrogen spillover. Facts and fiction, *Chem. Rev.*, 2012, **112**, 2714–2738.
13 F. Zaera, The long and winding road to catalysis, *Nature*, 2017, **541**, 37–38.
14 E. Lalik, S. F. Parker, G. Irvine, I. da Silva, M. J. Gutmann, G. Romanelli, K. Druzbicki, R. Kosydar and M. Krzystyniak, Hydrogen spillover in tungsten oxide bronzes as observed by broadband neutron spectroscopy, *Energies*, 2023, **16**, 5496.
15 K. Shun, K. Mori, S. Masuda, N. Hashimoto, Y. Hinuma, H. Kobayashi and H. Yamashita, Revealing hydrogen spillover pathways in reducible metal oxides, *Chem. Sci.*, 2022, **13**, 8137–8147.
16 M. Cargnello, V. V. T. Doan-Nguyen, T. R. Gordon, R. E. Diaz, E. A. Stach, R. J. Gorte, P. Fornasiero and C. B. Murray, Control of metal nanocrystal size reveals metal–support interface role for ceria catalysts, *Science*, 2013, **341**, 771–773.
17 Q. Fu, H. Saltsburg and M. Flytzani-Stephanopoulos, Active nonmetallic Au and Pt species on ceria-based water-gas shift catalysts, *Science*, 2003, **301**, 935–938.
18 T. Boningari, P. R. Ettireddy, A. Somogyvari, Y. Liu, A. Vorontsov, C. A. McDonald and P. G. Smirniotis, Influence of elevated surface texture hydrated titania on Ce-doped Mn/$TiO_2$ catalysts for the low-temperature SCR of $NO_x$ under oxygen-rich conditions, *J. Catal.*, 2015, **325**, 145–155.
19 G. X. Zhuang, Y. W. Chen, Z. Y. Zhuang, Y. Yu and J. G. Yu, Oxygen vacancies in metal oxides: recent progress towards advanced catalyst design, *Sci. China Mater.*, 2020, **63**, 2089–2118.
20 K. Yu, L. Lou, S. Liu and W. Zhou, Asymmetric oxygen vacancies: the intrinsic redox active sites in metal oxide catalysts, *Adv. Sci.*, 2020, **7**, 1901970.

21 W. Yang, F. Qi, W. An, H. Yu, S. Liu, P. Ma, R. Chen, S. Liu, L. Lou and K. Yu, Local electronic structure modulation of interfacial oxygen vacancies promotes the oxygen activation capacity of Pt/$Ce_{1-x}M_xO_{2-\delta}$, *ACS Catal.*, 2024, **14**, 5936–5948.

22 Z. Wu, W. Yin, B. Wen, D. Ma and L. Liu, Oxygen vacancy diffusion in rutile $TiO_2$: insight from deep neural network potential simulations, *J. Phys. Chem. Lett.*, 2023, **14**, 2208–2214.

23 F. Jiang, S. S. Wang, B. Liu, J. Liu, L. Wang, Y. Xiao, Y. B. Xu and X. H. Liu, Insights into the Influence of $CeO_2$ crystal facet on $CO_2$ hydrogenation to methanol over Pd/$CeO_2$ catalysts, *ACS Catal.*, 2020, **10**, 11493–11509.

24 Y. E. Kim, B. Kim, W. Lee, Y. N. Ko, M. H. Youn, S. K. Jeong, K. T. Park and J. Oh, Highly tunable syngas production by electrocatalytic reduction of $CO_2$ using Ag/$TiO_2$ catalysts, *Chem. Eng. J.*, 2021, **413**, 127448.

25 D. R. Aireddy and K. Ding, Heterolytic dissociation of $H_2$ in heterogeneous catalysis, *ACS Catal.*, 2022, **12**, 4707–4723.

26 S. Syrenova, C. Wadell, F. A. A. Nugroho, T. A. Gschneidtner, Y. A. D. Fernandez, G. Nalin, D. Switlik, F. Westerlund, T. J. Antosiewicz, V. P. Zhdanov, K. Moth-Poulsen and C. Langhammer, Hydride formation thermodynamics and hysteresis in individual Pd nanocrystals with different size and shape, *Nat. Mater.*, 2015, **14**, 1236–1244.

27 P. X. Liu, Y. Zhao, R. X. Qin, S. G. Mo, G. X. Chen, L. Gu, D. M. Chevrier, P. Zhang, Q. Guo, D. D. Zang, B. H. Wu, G. Fu and N. F. Zheng, Photochemical route for synthesizing atomically dispersed palladium catalysts, *Science*, 2016, **352**, 797–801.

28 Z. H. Zhang, Z. Q. Wang, Z. R. Li, W. B. Zheng, L. P. Fan, J. Zhang, Y. M. Hu, M. F. Luo, X. P. Wu, X. Q. Gong, W. X. Huang and J. Q. Lu, Metal-free ceria catalysis for selective hydrogenation of crotonaldehyde, *ACS Catal.*, 2020, **10**, 14560–14566.

29 C. Yang, S. Ma, Y. Liu, L. Wang, D. Yuan, W. Shao, L. Zhang, F. Yang, T. Lin, H. Ding, H. He, Z. Liu, Y. Cao, Y. Zhu and X. Bao, Homolytic $H_2$ dissociation for enhanced hydrogenation catalysis on oxides, *Nat. Commun.*, 2024, **15**, 540.

30 S. Xiang, L. Dong, Z. Wang, X. Han, L. L. Daemen, J. Li, Y. Cheng, Y. Guo, X. Liu, Y. Hu, A. J. Ramirez-Cuesta, S. Yang, X. Gong and Y. Wang, A unique Co@CoO catalyst for hydrogenolysis of biomass-derived 5-hydroxymethylfurfural to 2,5-dimethylfuran, *Nat. Commun.*, 2022, **13**, 3657.

31 S. Khoobiar, Particle to particle migration of hydrogen atoms on platinum—alumina catalysts from particle to neighboring particles, *J. Phys. Chem.*, 1964, **68**, 411–412.

32 M. Xiong, Z. Gao and Y. Qin, Spillover in heterogeneous catalysis: new insights and opportunities, *ACS Catal.*, 2021, **11**, 3159–3172.

33 M. Z. Li, W. A. Yin, J. A. Pan, Y. W. Zhu, N. Sun, X. Y. Zhang, Y. T. Wan, Z. Z. Luo, L. H. Yi and L. L. Wang, Hydrogen spillover as a promising strategy for boosting heterogeneous catalysis and hydrogen storage, *Chem. Eng. J.*, 2023, **471**, 144691.

34 S. Masuda, K. Shun, K. Mori, Y. Kuwahara and H. Yamashita, Synthesis of a binary alloy nanoparticle catalyst with an immiscible combination of Rh and Cu assisted by hydrogen spillover on a $TiO_2$ support, *Chem. Sci.*, 2020, **11**, 4194–4203.

35 M. D. Marcinkowski, A. D. Jewell, M. Stamatakis, M. B. Boucher, E. A. Lewis, C. J. Murphy, G. Kyriakou and E. C. H. Sykes, Controlling a spillover pathway with the molecular cork effect, *Nat. Mater.*, 2013, **12**, 523–528.

36 S. S. E. Collins, M. Cittadini, C. Pecharromán, A. Martucci and P. Mulvaney, Hydrogen spillover between single gold nanorods and metal oxide supports: a surface plasmon spectroscopy study, *ACS Nano*, 2015, **9**, 7846–7856.

37 R. A. Bennett, P. Stone and M. Bowker, Pd nanoparticle enhanced re-oxidation of non-stoichiometric $TiO_2$: STM imaging of spillover and a new form of SMSI, *Catal. Lett.*, 1999, **59**, 99–105.

38 Y. Lykhach, T. Staudt, M. Vorokhta, T. Skála, V. Johánek, K. C. Prince, V. Matolín and J. Libuda, Hydrogen spillover monitored by resonant photoemission spectroscopy, *J. Catal.*, 2012, **285**, 6–9.

39 J. VandeVondele, M. Krack, F. Mohamed, M. Parrinello, T. Chassaing and J. Hutter, QUICKSTEP: fast and accurate density functional calculations using a mixed Gaussian and plane waves approach, *Comput. Phys. Commun.*, 2005, **167**, 103–128.

40 C. Spreafico and J. VandeVondele, The nature of excess electrons in anatase and rutile from hybrid DFT and RPA, *PCCP*, 2014, **16**, 26144–26152.

41 Z. Tan, J. Chen and S. Lin, Theoretical insights into $H_2$ activation and hydrogen spillover on near-surface alloys with embedded single Pt atoms, *ACS Catal.*, 2024, **14**, 2194–2201.

42 M. Digne, P. Sautet, P. Raybaud, P. Euzen and H. Toulhoat, Use of DFT to achieve a rational understanding of acid–basic properties of γ-alumina surfaces, *J. Catal.*, 2004, **226**, 54–68.

43 R. Wischert, P. Laurent, C. Copéret, F. Delbecq and P. Sautet, γ-Alumina: the essential and unexpected role of water for the structure, stability, and reactivity of "defect" sites, *J. Am. Chem. Soc.*, 2012, **134**, 14430–14449.

44 M. J. Nash, A. M. Shough, D. W. Fickel, D. J. Doren and R. F. Lobo, High-temperature dehydrogenation of Bronsted acid sites in zeolites, *J. Am. Chem. Soc.*, 2008, **130**, 2460–2462.

45 M. Vitiello, N. Lopez, F. Illas and G. Pacchioni, $H_2$ cracking at $SiO_2$ defect centers, *J. Phys. Chem. A*, 2000, **104**, 4674–4684.

46 M. Ramos, A. E. Martínez and H. F. Busnengo, $H_2$ dissociation on individual Pd atoms deposited on Cu(111), *PCCP*, 2012, **14**, 303–310.

47 K. X. Gu, F. F. Wei, Y. H. Cai, S. Lin and H. Guo, Dynamics of initial hydrogen spillover from a single atom platinum active site to the Cu(111) host surface: the impact of substrate electron-hole pairs, *J. Phys. Chem. Lett.*, 2021, **12**, 8423–8429.

48 W. Osada, S. Tanaka, K. Mukai, M. Kawamura, Y. Choi, F. Ozaki, T. Ozaki and J. Yoshinobu, Elucidation of the atomic-scale processes of dissociative adsorption and spillover of hydrogen on the single atom alloy catalyst Pd/Cu(111), *PCCP*, 2022, **24**, 21705–21713.

49 K. Gu and S. Lin, Sustained hydrogen spillover on Pt/Cu(111) single-atom alloy: dynamic insights into gas-induced chemical processes, *Angew. Chem., Int. Ed.*, 2023, **62**, e202312796.

50 A. Mahdavi-Shakib, T. N. Whittaker, T. Y. Yun, K. B. Sravan Kumar, L. C. Rich, S. Wang, R. M. Rioux, L. C. Grabow and B. D. Chandler, The role of surface hydroxyls in the entropy-driven adsorption and spillover of $H_2$ on $Au/TiO_2$ catalysts, *Nat. Catal.*, 2023, **6**, 710–719.

51 S. Campisi, C. E. Chan-Thaw, L. E. Chinchilla, A. Chutia, G. A. Botton, K. M. H. Mohammed, N. Dimitratos, P. P. Wells and A. Villa, Dual-site-mediated hydrogenation catalysis on Pd/NiO: selective biomass transformation and maintenance of catalytic activity at low Pd loading, *ACS Catal.*, 2020, **10**, 5483–5492.

52 T. C. Xiao, X. H. Liu, G. Y. Xu and Y. Zhang, Phase tuning of $ZrO_2$ supported cobalt catalysts for hydrodeoxygenation of 5-hydroxymethylfurfural to 2,5-dimethylfuran under mild conditions, *Appl. Catal., B*, 2021, **295**, 120270.

53 J. Wei, S. N. Qin, J. L. Liu, X. Y. Ruan, Z. Q. Guan, H. Yan, D. Y. Wei, H. Zhang, J. Cheng, H. X. Xu, Z. Q. Tian and J. F. Li, *In Situ* raman monitoring and manipulating of interfacial hydrogen spillover by precise fabrication of Au/$TiO_2$/Pt sandwich structures, *Angew. Chem., Int. Ed.*, 2020, **59**, 10343–10347.

54 T. Ioannides and X. E. Verykios, The interaction of benzene and toluene with Rh dispersed on $SiO_2$, $Al_2O_3$, and $TiO_2$ carriers, *J. Catal.*, 1993, **143**, 175–186.

55 G. J. Zhang, F. Y. Tang, X. Wang, L. Q. Wang and Y. N. Liu, Atomically dispersed Co–S–N active sites anchored on hierarchically porous carbon for efficient catalytic hydrogenation of nitro compounds, *ACS Catal.*, 2022, **12**, 5786–5794.

56 C. L. Mao, J. X. Wang, Y. J. Zou, G. D. Qi, J. Y. Y. Loh, T. H. Zhang, M. K. Xia, J. Xu, F. Deng, M. Ghoussoub, N. P. Kherani, L. Wang, H. Shang, M. Q. Li, J. Li, X. Liu, Z. H. Ai, G. A. Ozin, J. C. Zhao and L. Z. Zhang, Hydrogen spillover to oxygen vacancy of $TiO_2$-*x*Hy/Fe: breaking the scaling relationship of ammonia synthesis, *J. Am. Chem. Soc.*, 2020, **142**, 17403–17412.

57 G. Sun, D. Liu, H. Shi, J. Li, L. Yang, F. Tian, Y. Cui, C. Wang, F. Li, T. Zhao, H. Zhu, B. Liu, Y. Chai, Y. Liu and Y. Pan, Oxygen-vacancy-induced built-in electric field across MoCo dual-atomic site catalyst for promoting hydrogen spillover in hydrocracking and hydrodesulfurization, *ACS Catal.*, 2024, **14**, 3208–3217.

58 Z. W. Wei, H. J. Wang, C. Zhang, K. Xu, X. L. Lu and T. B. Lu, Reversed charge transfer and enhanced hydrogen spillover in platinum nanoclusters anchored on titanium oxide with rich oxygen vacancies boost hydrogen evolution reaction, *Angew. Chem., Int. Ed.*, 2021, **60**, 16622–16627.

59 X. Zhao, J. Wang, L. Lian, G. Zhang, P. An, K. Zeng, H. He, T. Yuan, J. Huang, L. Wang and Y. Liu, Oxygen vacancy-reinforced water-assisted proton hopping for enhanced catalytic hydrogenation, *ACS Catal.*, 2023, **13**, 2326–2334.

60 N. B. A. Jr, H. Kasai, W. A. Diño and H. Nakanishi, Potential energy of $H_2$ dissociation and adsorption on Pt(111) surface: first-principles calculation, *Jpn. J. Appl. Phys.*, 2007, **46**, 4233.

61 F. P. Netzer and G. Kneringer, The adsorption of hydrogen and the reaction of hydrogen with oxygen on Pt (100), *Surf. Sci.*, 1975, **51**, 526–538.

62 B. Poelsema, K. Lenz and G. Comsa, The dissociative adsorption of hydrogen on defect-'free' Pt(111), *J. Phys.: Condens. Matter*, 2010, **22**, 304006.

63 M. M. Bettahar, The hydrogen spillover effect. A misunderstanding story, *Catal. Rev. Sci. Eng.*, 2022, **64**, 87–125.

64 S. Lee, K. Lee, J. Im, H. Kim and M. Choi, Revisiting hydrogen spillover in Pt/LTA: effects of physical diluents having different acid site distributions, *J. Catal.*, 2015, **325**, 26–34.

65 M. Tan, Y. Yang, Y. Yang, J. Chen, Z. Zhang, G. Fu, J. Lin, S. Wan, S. Wang and Y. Wang, Hydrogen spillover assisted by oxygenate molecules over nonreducible oxides, *Nat. Commun.*, 2022, **13**, 1457.

66 N. M. Zou, X. C. Zhou, G. Q. Chen, N. M. Andoy, W. Jung, G. K. Liu and P. Chen, Cooperative communication within and between single nanocatalysts, *Nat. Chem.*, 2018, **10**, 607–614.

67 M. F. de Lange, K. J. F. M. Verouden, T. J. H. Vlugt, J. Gascon and F. Kapteijn, Adsorption-driven heat pumps: the potential of metal–organic frameworks, *Chem. Rev.*, 2015, **115**, 12205–12250.

68 N. C. Burtch, I. M. Walton, J. T. Hungerford, C. R. Morelock, Y. Jiao, J. Heinen, Y. S. Chen, A. A. Yakovenko, W. Q. Xu, D. Dubbeldam and K. S. Walton, *In situ* visualization of loading-dependent water effects in a stable metal–organic framework, *Nat. Chem.*, 2020, **12**, 186–192.

69 Z. Gu, M. Li, C. Chen, X. Zhang, C. Luo, Y. Yin, R. Su, S. Zhang, Y. Shen, Y. Fu, W. Zhang and F. Huo, Water-assisted hydrogen spillover in Pt nanoparticle-based metal–organic framework composites, *Nat. Commun.*, 2023, **14**, 5836.

70 R. I. Cukier and D. G. Nocera, Proton-coupled electron transfer, *Annu. Rev. Phys. Chem.*, 1998, **49**, 337–369.

71 X. Li, X. M. Ren, M. Guo, W. J. Li and Q. H. Yang, Water accelerated activity of Ru NPs in sequential hydrogenation of nitrobenzene to cyclohexylamine, *J. Catal.*, 2022, **413**, 546–553.

72 Z. Zhao, R. Bababrik, W. H. Xue, Y. P. Li, N. M. Briggs, D. T. Nguyen, U. Nguyen, S. P. Crossley, S. W. Wang, B. Wang and D. E. Resasco, Solvent-mediated charge separation drives alternative hydrogenation path of furanics in liquid water, *Nat. Catal.*, 2019, **2**, 431–436.

73 Y. H. Dai, X. F. Chu, J. J. Gu, X. Gao, M. Xu, D. Lu, X. Y. Wan, W. Qi, B. S. Zhang and Y. H. Yang, Water-enhanced selective hydrogenation of cinnamaldehyde to cinnamyl

alcohol on RuSnB/$CeO_2$ catalysts, *Appl. Catal., A*, 2019, **582**, 117098.

74 R. Samanta, B. K. Manna, R. Trivedi, B. Chakraborty and S. Barman, Hydrogen spillover enhances alkaline hydrogen electrocatalysis on interface-rich metallic Pt-supported MoO, *Chem. Sci.*, 2023, **15**, 364–378.

75 Y. An, P. Chatterjee, P. Naik, S. Banerjee, W. Y. Huang, I. I. Slowing and V. Venditti, Hydrogen spillover and substrate-support hydrogen bonding mediate hydrogenation of phenol catalyzed by palladium on reducible metal oxides, *Chem. Sci.*, 2023, **14**, 14166–14175.

76 P. X. Liu, R. X. Qin, G. Fu and N. F. Zheng, Surface coordination chemistry of metal nanomaterials, *J. Am. Chem. Soc.*, 2017, **139**, 2122–2131.

77 N. Kaeffer, D. Mance and C. Copéret, N-Heterocyclic carbene coordination to surface copper sites in selective semihydrogenation catalysts from solid-state NMR spectroscopy, *Angew. Chem., Int. Ed.*, 2020, **59**, 19999–20007.

78 F. Zaera, CHEMISTRY the long and winding road to catalysis, *Nature*, 2017, **541**, 37–38.

79 S. Zhang, Z. Xia, M. Zhang, Y. Zou, H. Shen, J. Li, X. Chen and Y. Qu, Boosting selective hydrogenation through hydrogen spillover on supported-metal catalysts at room temperature, *Appl. Catal., B*, 2021, **297**, 120418.

80 S. C. Tsang, N. Cailuo, W. Oduro, A. T. S. Kong, L. Clifton, K. M. K. Yu, B. Thiebaut, J. Cookson and P. Bishop, Engineering preformed cobalt-doped platinum nanocatalysts for ultraselective hydrogenation, *ACS Nano*, 2008, **2**, 2547–2553.

81 Q. Zheng, H. Xu, Y. Yao, J. Dai, J. Wang, W. Hou, L. Zhao, X. Zou, G. Zhan, R. Wang, K. Wang and L. Zhang, Cobalt single-atom reverse hydrogen spillover for efficient electrochemical water dissociation and dechlorination, *Angew. Chem., Int. Ed.*, 2024, **63**, e202401386.

82 W. Liu, H. Feng, Y. Yang, Y. Niu, L. Wang, P. Yin, S. Hong, B. Zhang, X. Zhang and M. Wei, Highly-efficient RuNi single-atom alloy catalysts toward chemoselective hydrogenation of nitroarenes, *Nat. Commun.*, 2022, **13**, 3188.

83 C. Choi, X. Wang, S. Kwon, J. L. Hart, C. L. Rooney, N. J. Harmon, Q. P. Sam, J. J. Cha, W. A. Goddard, M. Elimelech and H. Wang, Efficient electrocatalytic valorization of chlorinated organic water pollutant to ethylene, *Nat. Nanotechnol.*, 2023, **18**, 160–167.

84 C. Han, J. Zenner, J. Johny, N. Kaeffer, A. Bordet and W. Leitner, Electrocatalytic hydrogenation of alkenes with Pd/carbon nanotubes at an oil–water interface, *Nat. Catal.*, 2022, **5**, 1110–1119.

85 G. Han, G. Li and Y. Sun, Electrocatalytic dual hydrogenation of organic substrates with a Faradaic efficiency approaching 200%, *Nat. Catal.*, 2023, **6**, 224–233.

86 D. Huang, D. J. Kim, K. Rigby, X. Zhou, X. Wu, A. Meese, J. Niu, E. Stavitski and J.-H. Kim, Elucidating the role of single-atom Pd for electrocatalytic hydrodechlorination, *Environ. Sci. Technol.*, 2021, **55**, 13306–13316.

87 M. Li and J. Shen, Microcalorimetric studies of $O_2$ and $C_2H_4$ adsorption on Pd/$SiO_2$ catalysts modified by Cu and Ag, *Thermochim. Acta*, 2001, **379**, 45–50.

88 H. Zhou, X. Yang, L. Li, X. Liu, Y. Huang, X. Pan, A. Wang, J. Li and T. Zhang, PdZn intermetallic nanostructure with Pd–Zn–Pd ensembles for highly active and chemoselective semi-hydrogenation of acetylene, *ACS Catal.*, 2016, **6**, 1054–1061.

89 F. Studt, F. Abild-Pedersen, T. Bligaard, R. Z. Sørensen, C. H. Christensen and J. K. Nørskov, Identification of non-precious metal alloy catalysts for selective hydrogenation of acetylene, *Science*, 2008, **320**, 1320–1322.

90 K. R. Kahsar, D. K. Schwartz and J. W. Medlin, Control of metal catalyst selectivity through specific noncovalent molecular interactions, *J. Am. Chem. Soc.*, 2014, **136**, 520–526.

91 K.-i. Shimizu, Y. Miyamoto, T. Kawasaki, T. Tanji, Y. Tai and A. Satsuma, Chemoselective hydrogenation of nitroaromatics by supported gold catalysts: mechanistic reasons of size-and support-dependent activity and selectivity, *J. Phys. Chem. C*, 2009, **113**, 17803–17810.

92 B. Wu, H. Huang, J. Yang, N. Zheng and G. Fu, Selective hydrogenation of α,β-unsaturated aldehydes catalyzed by amine-capped platinum-cobalt nanocrystals, *Angew. Chem., Int. Ed.*, 2012, **51**, 3440–3443.

93 Y. Li, Y. Zhang, K. Qian and W. Huang, Metal–support interactions in metal/oxide catalysts and oxide–metal interactions in oxide/metal inverse catalysts, *ACS Catal.*, 2022, **12**, 1268–1287.

94 D. X. Ji, L. Fan, L. Tao, Y. J. Sun, M. G. Li, G. R. Yang, T. Q. Tran, S. Ramakrishna and S. J. Guo, The kirkendall effect for engineering oxygen vacancy of hollow CoO nanoparticles toward high-performance portable zinc-air batteries, *Angew. Chem., Int. Ed.*, 2019, **58**, 13840–13844.

95 C. D. Lv, C. Lee, L. X. Zhong, H. J. Liu, J. W. Liu, L. Yang, C. S. Yan, W. Yu, H. H. Hng, Z. M. Qi, L. Song, S. Z. Li, K. P. Loh, Q. Y. Yan and G. H. Yu, A defect engineered electrocatalyst that promotes high-efficiency urea synthesis under ambient conditions, *ACS Nano*, 2022, **16**, 8213–8222.

96 C. Xie, D. F. Yan, H. Li, S. Q. Du, W. Chen, Y. Y. Wang, Y. Q. Zou, R. Chen and S. Y. Wang, Defect chemistry in heterogeneous catalysis: recognition, understanding, and utilization, *ACS Catal.*, 2020, **10**, 11082–11098.

97 Y. Lu, T. Liu, C.-L. Dong, C. Yang, L. Zhou, Y. Huang, Y. Li, B. Zhou, Y. Zou and S. Wang, Tailoring competitive adsorption sites by oxygen-vacancy on cobalt oxides to enhance the electrooxidation of biomass, *Adv. Mater.*, 2022, **34**, 2107185.

98 F. Zhang, B. Li, X. Quan, K. Wang, J. Xu, T. Wu, Z. Li, M. Yan, S. Liu, Y. He, Y. Shi, Y. Su and P. Xie, Revealing the dynamics of oxygen vacancy in $ZnO_{1-x}$/Cu during robust methanol synthesis from $CO_2$, *ACS Catal.*, 2024, **14**, 7136–7148.

99 G. Xiang, H. Chen, C. Yi, Z. Liu and S. Dai, Oxygen vacancy-regulated atomic dispersed Au on $CeFeO_x$ for preferential

oxidation of CO in $H_2$-rich stream, *Chem. Eng. J.*, 2024, **479**, 147775.

100 H. Xu, H. Zhang, L. Cui, X. Zhao, J. Xiao, J. Zhang, Y. Qin and J. Zhang, Unravelling the synergy of platinum-oxygen vacancy in $CoO_x$ for modulating hydrogenation performance, *Chem. Eng. J.*, 2024, **488**, 150841.

101 F. X. Zhang, B. Y. Li, X. Quan, K. Wang, J. Y. Xu, T. T. Wu, Z. L. Li, M. Yan, S. J. Liu, Y. He, Y. Shi, Y. Q. Su and P. F. Xie, Revealing the dynamics of oxygen vacancy in $ZnO_{1-x}$/Cu during robust methanol synthesis from $CO_2$, *ACS Catal.*, 2024, **14**, 7136–7148.

102 X. X. Wei, X. J. Wen, Y. Y. Liu, C. Chen, C. Xie, D. D. Wang, M. Y. Qiu, N. H. He, P. Zhou, W. Chen, J. Cheng, H. Z. Lin, J. F. Jia, X. Z. Fu and S. Y. Wang, Oxygen vacancy-mediated selective C–N coupling toward electrocatalytic urea synthesis, *J. Am. Chem. Soc.*, 2022, **144**, 11530–11535.

103 S. N. Jiang, N. Ji, X. Y. Diao, H. Y. Li, Y. Rong, Y. X. Lei and Z. H. Yu, Vacancy engineering in transition metal sulfide and oxide catalysts for hydrodeoxygenation of lignin-derived oxygenates, *ChemSusChem*, 2021, **14**, 4377–4396.

104 M. Yazdanpanah, M. Fereidooni, V. Marquez, C. V. Paz, T. Saelee, M. S. Villanueva, M. Rittiruam, P. Khajondetchairit, S. Praserthdam and P. Praserthdam, The underlying catalytic role of oxygen vacancies in fatty acid methyl esters ketonization over $TiO_2$ catalysts, *ChemSusChem*, 2024, **17**, e202301033.

105 P. Nikacevic, F. S. Hegner, J. R. Galán-Mascarós and N. López, Influence of oxygen vacancies and surface facets on water oxidation selectivity toward oxygen or hydrogen peroxide with $BiVO_4$, *ACS Catal.*, 2021, **11**, 13416–13422.

106 Q. Wang, R. Duan, Z. Feng, Y. Zhang, P. Luan, Z. Feng, J. Wang and C. Li, Understanding the synergistic catalysis in hydrogenation of carbonyl groups on Cu-based catalysts, *ACS Catal.*, 2024, **14**, 1620–1628.

107 Y. Sun, B. Du, Y. Wang, M. Zhang and S. Zhang, Hydrogen spillover-accelerated selective hydrogenation on WO3 with ppm-level Pd, *ACS Appl. Mater. Interfaces*, 2023, **15**, 20474–20482.

108 J. Zhang, M. Gao, R. Wang, X. Li, P. Zhu, Y. Wang and Z. Zheng, Oxygen vacancy regulated selective hydrogenation of α,β-unsaturated aldehydes over LDH surface group coordinated transition metal photocatalysts, *Catal. Sci. Technol.*, 2022, **12**, 6163–6173.

109 R. V. Jagadeesh, A.-E. Surkus, H. Junge, M.-M. Pohl, J. Radnik, J. Rabeah, H. Huan, V. Schünemann, A. Brückner and M. Beller, Nanoscale $Fe_2O_3$-based catalysts for selective hydrogenation of nitroarenes to anilines, *Science*, 2013, **342**, 1073–1076.

110 H. S. Wei, X. Y. Liu, A. Q. Wang, L. L. Zhang, B. T. Qiao, X. F. Yang, Y. Q. Huang, S. Miao, J. Y. Liu and T. Zhang, $FeO_x$-supported platinum single-atom and pseudo-single-atom catalysts for chemoselective hydrogenation of functionalized nitroarenes, *Nat. Commun.*, 2014, **5**, 5634.

111 T. Schwob and R. Kempe, A reusable Co catalyst for the selective hydrogenation of functionalized nitroarenes and the direct synthesis of imines and benzimidazoles from nitroarenes and aldehydes, *Angew. Chem., Int. Ed.*, 2016, **55**, 15175–15179.

112 L. Zhang, M. Zhou, A. Wang and T. Zhang, Selective hydrogenation over supported metal catalysts: from nanoparticles to single atoms, *Chem. Rev.*, 2020, **120**, 683–733.

113 A. Deshpande, F. Figueras, M. Lakshmi Kantam, K. Jeeva Ratnam, R. Sudarshan Reddy and N. S. Sekhar, Environmentally friendly hydrogenation of nitrobenzene to p-aminophenol using heterogeneous catalysts, *J. Catal.*, 2010, **275**, 250–256.

114 W. C. Cheong, W. J. Yang, J. Zhang, Y. Li, D. Zhao, S. J. Liu, K. L. Wu, Q. G. Liu, C. Zhang, D. S. Wang, Q. Peng, C. Chen and Y. D. Li, Isolated iron single-atomic site-catalyzed chemoselective transfer hydrogenation of nitroarenes to arylamines, *ACS Appl. Mater. Interfaces*, 2019, **11**, 33819–33824.

115 V. K. Das, S. Mazhar, L. Gregor, B. D. Stein, D. G. Morgan, N. A. Maciulis, M. Pink, Y. Losovyj and L. M. Bronstein, Graphene derivative in magnetically recoverable catalyst determines catalytic properties in transfer hydrogenation of nitroarenes to anilines with 2-propanol, *ACS Appl. Mater. Interfaces*, 2018, **10**, 21356–21364.

116 Y. Guo, M. Wang, Q. Zhu, D. Xiao and D. Ma, Ensemble effect for single-atom, small cluster and nanoparticle catalysts, *Nat. Catal.*, 2022, **5**, 766–776.

117 L. Jiang, K. Liu, S. Hung, L. Zhou, R. Qin, Q. Zhang, P. Liu, L. Gu, H. M. Chen, G. Fu and N. Zheng, Facet engineering accelerates spillover hydrogenation on highly diluted metal nanocatalysts, *Nat. Nanotechnol.*, 2020, **15**, 848–853.

118 M. J. Hülsey, V. Fung, X. Hou, J. Wu and N. Yan, Hydrogen spillover and its relation to hydrogenation: observations on structurally defined single-atom sites, *Angew. Chem., Int. Ed.*, 2022, **61**, e202208237.

119 V. Fung, G. Hu, Z. Wu and D.-e. Jiang, Hydrogen in nanocatalysis, *J. Phys. Chem. Lett.*, 2020, **11**, 7049–7057.